ELSEVIER

Contents lists available at ScienceDirect

Science of the Total Environment

journal homepage: www.elsevier.com/locate/scitotenv





Degradation of low-density polyethylene by the bacterium *Rhodococcus* sp. C-2 isolated from seawater

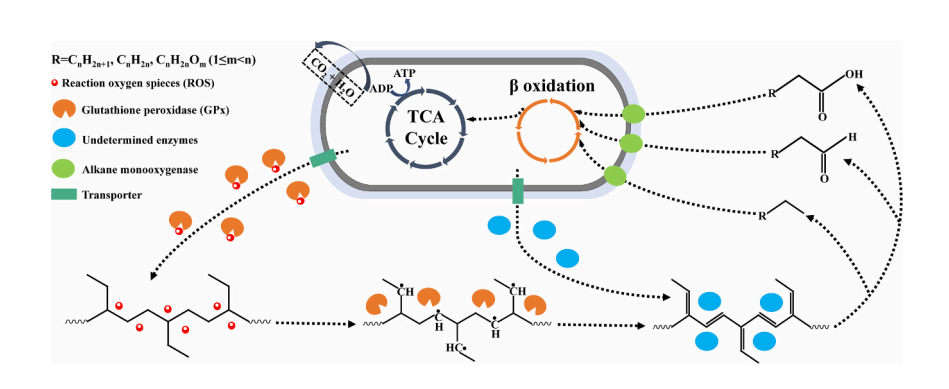
Zhen Rong, Zhi-Hao Ding, Yue-Hong Wu^{*}, Xue-Wei Xu^{*}

School of Oceanography, Shanghai Jiao Tong University, Shanghai 200240, PR China
Key Laboratory of Marine Ecosystem Dynamics, Ministry of Natural Resources & Second Institute of Oceanography, Ministry of Natural Resources, Hangzhou 310012,
PR China

HIGHLIGHTS

- Rhodococcus sp. C-2 was isolated from seawater after PE-degrading enrichment.
- Strain C-2 degraded LDPE film with higher efficiency than other bacteria in 30 d.
- The enzyme GPx depolymerized LPDE with the cooperation of its dissociated O₂[•].
- A multienzyme pathway was proposed to promote the understanding of PE degradation.

GRAPHICAL ABSTRACT



ARTICLE INFO

Editor: Fang Wang

Keywords: Biodegradation Low-density polyethylene Marine bacterium Glutathione peroxidase

ABSTRACT

Low-density polyethylene (LDPE), which accounts for 20% of the global plastic production, is discharged in great quantities into the ocean, threatening marine life and ecosystems. Marine microorganisms have previously been reported to degrade LDPE plastics; however, the exploration of strains and enzymes that degrade LDPE is still limited. Here, an LDPE-degrading bacterium was isolated from seawater of the Changjiang Estuary, China and identified as *Rhodococcus* sp. C-2, the relative abundance of which was dramatically enhanced during PE-degrading microbial enrichment. The strain C-2 exhibited the degradation of LDPE films, leading to their morphological deterioration, reduced hydrophobicity and tensile strength, weight loss, as well as the formation of oxygen-containing functional groups in short-chain products. Sixteen bacterial enzymes potentially involved in LDPE degradation were screened using genomic, transcriptomic, and degradation product analyses. Thereinto, the glutathione peroxidase GPx with exposed active sites catalyzed the LDPE depolymerization with the cooperation of its dissociated superoxide anion radicals. Furthermore, an LDPE degradation model involving multiple enzymes was proposed. The present study identifies a novel PE-degrading enzyme (PEase) for polyethylene bioremediation and promotes the understanding of LDPE degradation.

E-mail addresses: yuehongwu@sio.org.cn (Y.-H. Wu), xuxw@sio.org.cn (X.-W. Xu).

^{*} Corresponding authors.

1. Introduction

By 2021, an estimated 75-199 million tons of plastic are projected to enter the ocean, with plastic waste accounting for a staggering 85% of the total marine litter (UNEP, 2021). Low-density polyethylene (LDPE) plastic accounts for approximately 20% of global plastic waste and is responsible for widespread marine plastic pollution (Geyer et al., 2017). In the ocean, the LDPE breaks down into debris (particle size >5 mm) or microplastics (particle size <5 mm) after exposure to ultraviolet radiation and mechanical weathering (Andrady, 1990; Andrady, 2011; Gall and Thompson, 2015). Large quantities of plastic debris and microplastics generally float on the sea surface owing to their low densities (0.917–0.930 g/cm³) (Schwarz et al., 2019). Consequently, they affect the marine ecosystem by enmeshing marine animals (Galgani et al., 2018), destroying habitat (Wang et al., 2019), facilitating biological invasion (García-Gómez et al., 2021) and absorbing toxic pollutants (Amelia et al., 2021), which threatens marine life and impact marine carbon cycles (Galgani and Loiselle, 2021). These ecological impacts are growing with plastic emissions into the ocean, and it is predicted that plastic waste, including LDPE, will continue to accumulate in the ocean with an increase of one order of magnitude in the next five years (Jambeck et al., 2015). The predicted statistic highlights the urgent need for effective measures to reduce plastic waste and prevent further damage to marine life.

Biodegradation refers to the process that breakdown of plastic polymers catalyzed by enzymes in vitro or in vivo (Duffus, 1993; Nagel et al., 1992). The biodegradation of plastics is an environmentally sound treatment that produces nonhazardous by-products (Moharir and Kumar, 2019). Polyethylene (PE) plastic possesses an extensive inert C-C backbone structure, devoid of any functional groups, thereby rendering it resistant to enzymatic degradation in the majority of organisms and thus classified as non-biodegradable (Ballerstedt et al., 2021). However, previous investigations have identified PE-degrading microorganisms from both soil and insect gut environments, typically forming robust biofilms on the surface of polyethylene (Montazer et al., 2019; Yang et al., 2014). With the advancement of research on plastic pollution in the ocean, it has been discovered that biofilms usually develop on PE plastic debris in the ocean, and microbes dwelling within these plastic biofilms are capable of utilizing PE as a source of carbon and energy in situ (Montazer et al., 2020; Pinto et al., 2022; Tsiota et al., 2018). Theoretically, it is feasible to isolate microbes from marine regions contaminated with plastic in order to facilitate the biodegradation of LDPE. In fact, marine bacteria and fungi found in areas with plastic pollution or on plastic fragments have demonstrated significant ability to degrade LDPE. Based on the morphological and physicochemical changes detected in plastics, several marine bacteria strains have been confirmed for their ability to degrade LDPE (Harshvardhan and Jha, 2013; Khandare et al., 2021; Kumari et al., 2019; Li et al., 2020; Sudhakar et al., 2008). Among them, Bacillus sphericus isolated from shallow waters of the Indian Ocean has exhibited the most effective degradation capability by reducing plastic weight by up to 10% within a year (Sudhakar et al., 2008). Futhermore, marine fungi, such as Aspergillus terreus (Ameen et al., 2015) and Penicillium sp. (Alshehrei, 2017), also play a significant role in the degradation of LDPE. The most efficient marine fungus, Alternaria alternata FB1, is able to reduce the average molecular weight of an LDPE film by 95% within a period of 120 days (Gao et al., 2022). The presence of LDPE-degrading microorganisms significantly accelerate the degradation process of LDPE, in comparison to its natural weathering half-life in the ocean (ca. 1.4-2500 years) (Chamas et al., 2020). The untapped potential of marine microorganisms in degrading PE is significant and warrants further exploration.

Previous studies have suggested that microbial degradation of PE roughly involves four main processes, namely colonization, depolymerization, assimilation, and mineralisation (Gao et al., 2022; Restrepo-Flórez et al., 2014; Yuan et al., 2020). Certain abiotic factors such as UV and heat can facilitate the biodegradation process of PE (Auta et al.,

2018; Balasubramanian et al., 2014; Gilan (Orr) et al., 2004; Mohanan et al., 2020; Volke-Sepúlveda et al., 2002). However, the exact pathway of PE biodegradation is still not fully explored (Danso et al., 2019). The biodegradation of PE polymers is primarily caused by the depolymerization of long carbon chains, and this process involves the breaking of C-C bonds with the catalysis of microbial enzymes, which also introduce oxygen into the polymer structure (Ghatge et al., 2020). Currently, there is limited research on the detection and characterization of PEases. To date, only a handful of enzymes have been identified from microbes as capable of degrading PE polymers, including alkane monooxygenase (Yoon et al., 2012), laccase (Gao et al., 2022; Santo et al., 2013; Yao, C. et al., 2022), glutathione peroxidase (Gao et al., 2022), manganese peroxidase (Ehara et al., 2000; Iiyoshi et al., 1998) and lignin peroxidase (Mukherjee and Kundu, 2014). Research has shown that alkane monooxygenase (AlkB) is capable of decomposing polyethylene with low average molecular weight (Mw <30,000) through terminal or subterminal oxidation (Restrepo-Flórez et al., 2014). By comparison, certain laccases and peroxidases have been proven to effectively degrade high molecular weight polyethylene (Mw >100,000) (Gao et al., 2022; Santo et al., 2013; Zhang et al., 2023). The degradative activities of laccases and manganese peroxidases are associated with metal ions, whose presence promote enzymatic activity (Iiyoshi et al., 1998; Santo et al., 2013; Zhang et al., 2022). So far, there is still a lack of in-depth studies on glutathione peroxidase and lignin peroxidase, leaving their reaction processes and degradation products unclear. The precise function of PEases in the microbial metabolism of polyethylene requires further investigation.

In the present study, the PE-degrading bacterium *Rhodococcus* sp. C-2 was isolated using a multi-stage enrichment culture from a seawater sample from the Changjiang Estuary, which has a high abundance of suspended plastic debris during summer (Peng et al., 2017; Xu et al., 2018; Zhang et al., 2019; Zhao et al., 2019). Furthermore, multiple technologies were used to verify the degradation capacity and by-products of strain C-2 on LDPE films. Transcriptome analysis revealed mutiple bacterial enzymes potentially associated with the LDPE degradation process and a glutathione peroxidase was heterologously expressed, verifying the LDPE-degrading capacity in vitro. Moverover, a metabolic pathway was proposed to describe the process of LDPE biodegradation by strain C-2.

2. Materials and methods

2.1. PE materials

Two PE materials were used as the carbon source for the biodegradation assay: PE powders (427772, Sigma-Aldrich Company, USA) and LDPE films (0.25 mm thick, ET311350, Good Fellow Company, UK). The number average molecular weight (Mn) and weight average molecular weight (Mw) of PE powders were 1700 and 4000, respectively. The Mw and Mn of LDPE films are characterized by high temperature gel permeation chromatography (HT-GPC, HLC-8321GPC/HT, TOSOH, Japan) using 1, 2-dichlorobenzene (D108133, Shanghai Aladdin Biochemical Technology Co., Ltd., China) as mobile phase with polystyrene standards (05202-05221, TOSOH, Japan). To prevent potential interference from additives in LDPE material on subsequent weight measurements, the purity of LDPE film is analyzed using a method of precipitation after dissolution in toluene (Wong et al., 2014). Briefly, pristine LDPE film is preweighted and then dissolved in toluene (650579, Sigma-Aldrich Company, USA) at 130 °C. After cooling down to room temperature, the extremely low molecular weight portion and the oxidized additives of LDPE are removed while pure LDPE is precipitated (Jeon and Kim, 2013). The precipitated LDPE is weighted, and the purity of LDPE film is calculated by the formula modified from the impurities extracted yield (Castro Issasi et al., 2019): 100% × (initial weight - precipitated weight) / initial weight. As the carbon source, PE powders (0.1–0.8 mm in diameter) and LDPE films (ca. 30×20 mm)

were washed with 75% ethanol. Thereafter, they were air-dried and weighed in a vertical flow clean bench before placing them in liquid medium.

2.2. Media and culture conditions

Carbon free marine (CFM) medium was modified from liquid carbon-free basal medium (LCFBM) (Yang et al., 2014) and contained 1 L deionized water, 1 g NH₄Cl, 1 g KH₂PO₄, 1 g K₂HPO₄·3H₂O, 0.2 g MgSO₄·7H₂O, 20 g NaCl, 0.001 g FeSO₄·7H₂O, 0.001 g ZnSO₄·7H₂O, 0.001 g MnSO₄·H₂O, 0.001 g CuSO₄·5H₂O and 0.1% vitamin solution (1 g nicotinic acid, 1 g thiamine hydrochloride, 0.05 g biotin, 0.5 g 4-aminobenzoic acid, 0.5 g vitamin B6, 0.01 g vitamin B12, 0.5 g calcium pantothenate, 0.5 g folic acid and 1 L deionized water) at pH 7.0. On the basis of CFM medium, low carbon marine (LCM) medium was modified by adding 0.5 g/L yeast extract and 1 g/L peptone (Gao et al., 2022; Gao and Sun, 2021). The reagents used in the above medium were purchased from Sangon Biotech (Shanghai) Co., Ltd., China. Marine broth 2216 and marine agar 2216 (BD Difco, UK) were used to isolate and purify the PE-degrading strain. All the culture assays were incubated aerobically on a rotary shaker at 30 °C.

2.3. Sample collection

Surface seawater and sediment samples were collected from the Changjiang Estuary and East China Sea, China. These samples were collected during a voyage in July 2020. Fig. S1 shows the 57 stations that were positioned at different locations throughout area covered during the voyage. Different sampling and processing procedures were used for seawater and sediment samples (Fig. S2). At sampling stations, 400-700 L of surface seawater (0-1 m from the surface) were pumped by immersible pump, which was then filtered through metal meshes of different aperture sizes of 500 mm, 2 mm, 280 μm and 74 μm , in turn. The particles on these meshes were flushed by seawater and then concentrated on a 0.22 µm nylon filter membrane (Millipore, USA). Surface sediment samples were collected using a bottom sampler (PSC-400A, China) and scraped from the top layer (0–5 cm below the seabed) using a disinfected scoop. The depth of each station is shown in Table S2. Filter membranes and sediment samples were immediately placed in sterile PE bags (Whirl-Pak, Nasco, USA) and stored at 4 °C until further analysis.

2.4. Enrichment and isolation of PE-degrading bacteria

2.4.1. Experimental design of enrichment

The entire enrichment process lasted 90 days and was divided into three stages: primary, secondary, and tertiary cultures (Kim et al., 2017). A seawater filter membrane or 1 g of sediment sample from each station were mixed with 20 mL of sterile 0.85% NaCl solution, and two mixtures were both shaken at 180 rpm for 3 h. Thereafter, 100 μ L of each mixture suspension was pipetted into a test tube ($\Phi18\times180$ mm) containing 10 mL CFM medium with 0.1 g PE powders for primary culture (Culture-1). Same mediums (CFM supplemented with PE) inoculated with 0.85% NaCl solution were used as controls. The primary culture was shaken at 30 °C and 160 rpm for 30 days. Thereafter, 1 mL primary culture samples were inoculated to a 100 mL CFM medium with 0.5 g PE powders for 30-day secondary culture (Culture-2) at 30 °C and 160 rpm. Using the samples after secondary culture, the same inoculation and culture procedure was performed for 30-day tertiary culture (Culture-3) under the conditions consistent with the secondary culture.

2.4.2. Surface morphology observation of PE powders

At the end of each culture stage, the surface morphology of the PE powders in the medium was observed by scanning electron microscopy (SEM) (Yoshida et al., 2016). Specifically, the PE powders in each sample were collected from the culture medium and immediately soaked

in 2% glutaraldehyde for 1 h, followed by rinsing in 100 mM phosphate buffered saline (pH 7.0) thrice (20 min each time). The cleaned PE powders were fixed with 2% osmic acid for 1 h, dehydrated with 30–100% graded ethanol for 15 min each, and further dried with CO_2 at the critical point. After sputtering a layer of gold onto the dehydrated PE powders, surface morphology images were obtained using a field-emission scanning electron microscope (HITACHI S-3000 N, Japan).

2.4.3. 16S rRNA gene amplicon sequencing-based analysis of enriched samples

At the end of each culture stage, 2 mL of culture samples were evenly mixed with the culture medium, and the PE powders were centrifuged at 10, 000 rpm for 10 min to collect the precipitate. Total DNAs was extracted from the precipitated samples using an SDS-based DNA extraction method (Natarajan et al., 2016). The hypervariable V4 regions of the prokaryotic 16S rRNA gene were amplified using primers (5'-GTGYCAGCMGCCGCGGTAA-3') and 806R (5'-GGAC-TACHVGGGTWTCTAAT-3'). The PCR products were detected and purified using 2% agarose gel electrophoresis. After recovery using the MinElute Gel Extraction Kit (OIAGEN GmbH, Germany), the amplicon products of each sample were sequenced using a paired-end sequencing strategy (PE250) on an Illumina NovaSeq6000. The raw data for each sample were analyzed using USEARCH and VSEARCH open-source software based on multiple procedures, including double-ended sequence splicing, quality control, redundant sequence removal, chimera detection and removal, species clustering, and taxonomic annotation (Rognes et al., 2016). The generated files were imported into R Studio (version 4.2.0), and bacterial community composition was determined at different stages using ggplot2 (v3.3.5). The relative species abundance of the samples was normalized using Pheatmap (version 1.0.12) to determine changes in microbiota composition at different stages.

2.4.4. Identification of PE-degrading strain C-2

Potential PE-degrading bacteria were isolated from tertiary culture samples. To isolate pure bacterial strains, the enriched culture was spread on marine agar 2216 plate by serially dilution and colonies were formed by incubation for 2–3 d at 30 $^{\circ}$ C. Colonies were selected and purified by repeated streaking. The purified isolates were incubated in marine broth 2216 in a rotary shaker incubator at 30 °C for 1-2 d to reach mid-log phase. Subsequently, 1% (v/v) cultures were transferred into a test tube (Φ 18 \times 180 mm) containing 10 mL CFM medium with 0.1 g PE powders. An equivoluminal medium of CFM inoculated with the corresponding strain was used as a negative control. All the assays were incubated at 30 °C and 160 rpm in triplicate. Bacterial growth was measured at an optical density of 600 nm (OD₆₀₀) using a spectrometer (Genesys 50, Thermo Scientific, USA). Depending on whether the strain was grown in CFM amended with PE powder, a strain capable of degrading PE (designated as C-2) was successfully obtained. The near full-length 16S rRNA genes of the pure strain were amplified using the 27F (AGAGTTTGATCMTGGCTCAG) and 1492R (TACGGTTACCTTGT-TACGACTT) universal primers (Polz and Cavanaugh, 1998) and sequenced by Sanger sequencing. The 16S rRNA gene sequences were aligned against the EzBioCloud 16S database (Yoon et al., 2017) to identify similarities with previously published species.

2.5. Biodegradation of LDPE film by strain C-2

2.5.1. Biodegradation experimental design

The LDPE degradability of strain C-2 was detected by incubation in LCM medium supplemented with LDPE films. When the optical density of strain C-2 reached approximately 0.8 (OD $_{600}$) in marine broth 2216, the cells were harvested by centrifugation at 8000 rpm and resuspended in an equal volume of saline as seeded cells. Then, 1 mL of seeded cells was inoculated into 100 mL of LCM medium with a piece of pre-weighed LDPE film (30 \times 20 mm, ca. 147 mg). Under equal conditions, the

medium inoculated with *Escherichia coli* BL21 (DE3) served as negative control and the medium without bacterial inoculation served as control. All treatments were carried out in triplicate and cultured in a shaker (30 $^{\circ}$ C and 100 rpm) for 30 days.

2.5.2. SEM and Atomic Force Microscope (AFM) observations

At the end of the 30-day incubation period, LDPE films were collected from the culture medium and immediately soaked in 5% glutaraldehyde for 1 h, rinsed in 100 mM phosphate-buffered saline (pH 7.0), dehydrated with 30-100% graded ethanol for 15 min each, and finally dried with CO2 at the critical point (Dey et al., 2020; Gao and Sun, 2021). Dehydrated LDPE were sputter-coated with a layer of gold using a sputter coater (MSP-1S, SHINKKU VD, Japan), and images were captured using a field-emission scanning electron microscope (FESEM, TM 1000, Hitachi, Japan). Additionally, to assess the alterations in surface topography of LDPE following biodegradation, the treated LDPE was subjected to 2% SDS solution, shaken at 60 rpm for 2 h, followed by rinsing with sterile water to eliminate biofilm and overnight drying in a sterile room. The surface damage of the dry LDPE film was determined in a two-dimensional manner using SEM above, while its surface topological changes were visualized and analyzed through AFM (nanoIR2 FS, Anasys, USA).

2.5.3. Weight loss analysis

After 30 days of incubation, the LDPE films in the culture medium were collected and treated with 2% SDS solution, shaken at 60 rpm for 2 h, and rinsed adequately with sterile water to remove biofilms. The cleaned LDPE films were air dried overnight in a sterile room. Finally, the residual LDPE films were weighed, and the weight loss percentage was calculated as (initial weight - final weight) / initial weight \times 100%.

2.5.4. HT-GPC analysis

HT-GPC (EcoSEC HLC-8321GPC/HT, TOSOH, Japan) was used to analyse the Mw, Mn, and molecular weight distribution (MWD) of LDPE film. After 30-day incubation and removal of the biofilm as described above, the residual LDPE film was weighed 20 mg and dissolved in 10 mL tetrahydrofuran (0.2%, w/v). The detection process was performed at 145 °C using 1, 2-dichlorobenzene as the mobile phase and calibrated using monodisperse polystyrene standards. By converting the elution time to logMw, the GPC curve is expressed as dWt/d(logMw) versus logMw, where Wt is the cumulative amount of solute eluted to the corresponding molecular weight.

2.5.5. Water contact angle (WCA) analysis

The contact angle serves as an indicator of the LDPE surface's hydrophobicity or wettability. In general, a water contact angle below 90° indicates the hydrophilic nature of the solid surface, whereas a water contact angle exceeding 90° suggests its hydrophobicity (Law, 2014). The analysis was conducted on samples placed on a glass slide using Optical Contact Angle Measuring Device (OCA-20, Dataphysics, Germany). Double Distilled water was used as the wetting liquid. The calculations were derived by averaging five measurements taken at appropriate intervals.

2.5.6. Tensile strength analysis

The rectangular specimens, measuring 1×3 cm, were precisely cut from the center of each LDPE samples using a manual cutting press (Zwick ZCP 020, Germany) and subsequently subjected to tensile strength testing. The tensile properties of the samples were evaluated using a universal material testing machine (Zwick/Roell Z020, Germany) under controlled conditions of 25 °C, 50% humidity, and crosshead speed of 25 mm/min (Sudhakar et al., 2008).

2.5.7. Attenuated total reflection-Fourier transformed infrared spectroscopy (ATR-FTIR) analysis

After 30 days of incubation and removal of the surface biofilms, the

dried LDPE films were analyzed to evaluate the modification of the functional groups in LDPE using ATR-FTIR (Nicolet iS5, Thermo Scientific, USA). The absorbance was measured over a wavelength range of 4000–450 cm $^{-1}$ at a resolution of 4 cm $^{-1}$ using OMNIC software (v7.3). The absorption peaks in the IR spectra indicate the methylene at the vicinity of 1465 cm $^{-1}$, ester carbonyl bond at the vicinity of 1740 cm $^{-1}$, keto carbonyl bond at the vicinity of 1715 cm $^{-1}$, internal double bond at the vicinity of 910 cm $^{-1}$ and terminal double bond (vinyl) at the vicinity of 910 cm $^{-1}$ respectively (Albertsson et al., 1987). Therefore, Ester Carbonyl Bond Index (ECBI = A1715/1465), Keto Bond Index (KCBI = A1715/1465), Internal Double Bond Index (IDBI = A1650/1465) and Vinyl Bond Index (IDBI = A910/1465) were calculated to evaluate the concentration of carbonyl groups and carbon-carbon double bonds (Sudhakar et al., 2008).

2.5.8. Gas chromatography-mass spectrometry (GC-MS) analysis

The products of the LDPE film released into the medium after degradation by strain C-2 were detected by GC-MS. Three experimental groups were designed as: (1) CFM medium (100 mL) + Strain C-2 $(OD_{600} = 0.3) + 10 \text{ g/L Glucose}; (2) \text{ CFM medium } (100 \text{ mL}) + \text{Strain C-2}$ $(OD_{600} = 0.3) + LDPE (30 \times 20 \text{ mm}); (3) CFM \text{ medium } (100 \text{ mL}) + 10 \text{ g/}$ L Glucose + LDPE (30 \times 20 mm). All treatments were cultivated at 30 $^{\circ}$ C for 30 days and performed in triplicate. Then, all cultures were centrifuged to collect the supernatant at 12,000 rpm and 4 $^{\circ}$ C for 30 min. Plastic degradation products were extracted by ethyl acetate and dichloromethane successively. First, the supernatant was extracted with an equal volume of ethyl acetate for 2 h and collect the first extract and supernatant. Subsequently, the supernatant was extracted again using dichloromethane in the same manner. All extract was dried using nitrogen gas and redissolved in 1 mL solvent mixed by dichloromethane and methanol (1:1). Then, 10 μL sample was injected in Focus DSQ II GC-MS system equipped with a TG-5 ms (30 m long, 0.25 mm internal diameter and 0.25 µm thickness) chromatographic column. The injection port was maintained at 270 °C. During operation, the column temperature was held for 4 min at 50 °C, then raised to 270 °C at 20 °C rise per min, and finally held for 15 min at 270 $^{\circ}$ C. The flow rate was set at 1 mL/min. Helium was used as the carrier gas. Ions/fragments were monitored in scanning mode at 40-600 Amu (Gao et al., 2022). Potential degradation products were identified by matching them with compounds in the NIST library.

2.6. Genomic and phylogenetic analysis of strain C-2

Strain C-2 was grown in 2216 broth for 2 days, and the cells were collected by centrifugation at 8000 rpm for 15 min. The genomic DNA of strain C-2 was extracted using a DNeasy Blood and Tissue Kit (Qiagen, Germany), and subsequent sequencing was performed using an Illumina PE150 by Tianjin Novogene Technology Co., Ltd. Raw read data were filtered using Fastp (Chen et al., 2018) and the genome was assembled using clean paired-end data from SPAdes 3.13.1 (Bankevich et al., 2012). CheckM was used to evaluate completeness and contamination of the assembled genome (Parks et al., 2015). Functional prediction and annotation of the genome were performed using Prokka 1.14.6 (Seemann, 2014). A core-genome phylogeny was generated using 17 representative genome-sequenced members of the genus Rhodococcus and a member of the genus Antrihabitans as an outgroup. A maximumlikelihood phylogenomic tree was reconstructed using IQ-Tree software (version 1.6.1) (Nguyen et al., 2015) and visualized using iTOL (Letunic and Bork, 2021).

2.7. Transcriptomic analysis of LDPE biodegradation by strain C-2

To screen for genes related to LDPE degradation, strain C-2 was cultivated in LCM medium with an LDPE film at 30 °C and 100 rpm, which served as the experimental group. Same culture without LDPE film was used as control group, and both groups were cultured in

triplicate. The growth of strain C-2 in the experimental group and the control group was measured at an optical density of 600 nm (OD₆₀₀) using a spectrometer (Genesys 50, Thermo Scientific, USA). After cultivation, each culture was centrifuged at 4 °C to harvest the cells, respectively. Total RNA from each group was extracted using TRIzol reagent (Invitrogen, USA). RNA integrity and concentration were assessed using 1% agarose gel electrophoresis and NanoDrop 2000 (Thermo Scientific). After ribosomal RNA was removed using the Ribooff rRNA Depletion Kit (Vazyme Biotech Co., Ltd.), a sequencing library was constructed using the RNAseq Library Prep Kit (KAITAI-BIO) and sequenced on the Illumina Novaseq 6000 platform. Sequencing was performed by Hangzhou Kaitai Biotechnology Co. Ltd. Raw data were filtered using Fastp to remove adapters, reads shorter than 50 bp, and low-quality bases (quality score < 20). The resulting clean data were aligned to the R. qingshnegii strain C-2 reference genome using Hisat2, and the level of gene expression was assessed by counting the reads mapped to the genome. Differential expression analysis between the control and experimental groups was performed using edgeR 3.40.1. The sum of mapping reads >10 in the two groups (*P* value <0.05) was used as a threshold to define differentially expressed genes. The fold change (FC) represents the ratio of expression level of experimental group to control group, and the absolute value of log₂FC >0.5 was used as the screening criterion for up-regulated or down-regulated genes.

2.8. LDPE degradation capacity verification and product analysis of glutathione peroxidase (GPx)

2.8.1. Quantitative reverse transcription PCR

To verify the upregulatory effect of the GPx gene (Gene ID: Rhq_00887) at the mRNA level after 30-day degradation of LDPE degradation by strain C-2, the relative gene abundance was detected by quantitative reverse transcription PCR using 16S rRNA as the internal reference gene. Target genes were amplified from the complementary DNA template of strain C-2 using the SYBR Green Pro Taq HS Premix (Accurate Biotechnology (Hunan) Co., LTD, China) with the corresponding primers (Table S1). Fluorescence signal accumulation was used to monitor the entire PCR process in real time and was converted into amplification and melting curves. The initial amounts of the target genes were quantitatively analyzed using a standard curve. The fold change (FC) of mRNA expression level was calculated using the $2^{-\Delta\Delta Ct}$ method (Schmittgen and Livak, 2008).

2.8.2. Multiple sequence alignment and structure prediction

The amino acid sequence of GPx was compared using BLASTP program against UniProtKB/Swiss-Prot database to find homologous sequences. High-identity amino acid sequences were selected for subsequent analysis combined with GPx. Multiple sequence alignment was performed using Clustal X version 2 and visualized using ESPript 3.0 (Robert and Gouet, 2014). The three-dimensional structure of GPx was predicted using the AlphaFold2 in Colab (Jumper et al., 2021; Mirdita et al., 2022), and structural characteristics were analyzed using Open-Source PyMOL version 2.4.0 (Schrödinger, 2020).

2.8.3. Heterologous expression and purification

The GPx gene was amplified from the genomic DNA of strain C-2 using $2\times$ Rapid Taq Master Mix (P222-01, Vazyme Biotech Co., Ltd., China) with the primers (F: TCCCATATGACAACTCCAGTACAGAACAT; R: TCGAAGCTTCTAGTTCTTGGGAAGCGC; the underlined sections indicate the restriction endonuclease sites NdeI and HindIII). The PCR product was purified using a Gel&PCR Clean-Up Kit (OMEGA, USA) and digested with NdeI/HindIII (Thermo Fisher Scientific, USA). Using T4 DNA ligase (Thermo Fisher Scientific), DNA fragments were ligated into the expression plasmid pET-28b (+) using a His-tag. The recombinant plasmid was transformed into E. coli DH5 α cells (TransGen Biotech, China) for plasmid replication and sequencing. The recombinant plasmid with the correct sequencing of the GPx gene was then

transformed into E. coli BL21 (DE3) cells (TransGen Biotech, China) for overexpression, followed by purification by metal chelate affinity chromatography. The theoretical isoelectric point (pI) and Mw of protein GPx was predicted by Compute pI/Mw tool in Expasy (https://web. expasy.org/compute_pi/). The recombinant strain was inoculated in LB medium supplementing kanamycin (50 µg/mL) and incubated in a rotating shaker at 37 °C and 180 rpm. The His-tagged protein was induced with 0.2 mM isopropyl-1-thio-β-D-galactopyranoside (ITPG) after the OD_{600} of cells reaching 0.6. The recombinant strain was continued to be cultured at 16 $^{\circ}\text{C}$ for 20 h and centrifuged to collect cells at 8000 rpm for 10 min. E. coli BL21 (DE3) cells were resuspended on ice in binding buffer (10 mM imidazole, 20 mM Tris-HCl, 500 mM NaCl, pH 8.0), ultrasonically cracked, and centrifuged at 12,000 rpm for 30 min. The supernatant was incubated with the Ni Sepharose High Performance reagent (GE Healthcare) for 30 min before elution. Subsequently, the protein-binding Ni Sepharose was washed with binding and washing buffers (50 mM imidazole, 20 mM Tris-HCl, 500 mM NaCl, pH 8.0). The His-tagged fusion proteins were eluted with elution buffer (250 mM imidazole, 20 mM Tris-HCl, and 500 mM NaCl, pH 8.0) and the eluted proteins were detected using 12% SDS-PAGE. The collected eluates of the target proteins were dialysed twice against dialysis buffer (20 mM Tris-HCl and 500 mM NaCl, pH 8.0) for 8 h to remove the imidazole. After filtration through 0.22 µm filter membrane, the concentration of GPx was measured using the BCA Protein Assay Kit (TaKaRa, Japan).

2.8.4. Determination of glutathione peroxidase activity

The activity of glutathione peroxidase was determined using kits purchased from Sangon Biotech (Shanghai) Co., Ltd. (China). All measurements were conducted in accordance with the manufacturer's instructions. GPx facilitates the oxidation of reduced glutathione (GSH) by $\rm H_2O_2$, resulting in the production of oxidized glutathione (GSSG). The compound formed by GSH and DTNB exhibits a characteristic absorption peak at 412 nm. The reduction in absorbance at 412 nm can serve as an indicator of glutathione peroxidase activity. The enzyme activity unit is defined as the catalysis of 1 nmol GSH oxidation per mg protein per minute in the reaction system.

2.8.5. Characterization of LDPE biodegradation activity and products

The degradation experiment was designed as 4 mL reaction system containing reaction buffer (20 mM Tris-HCl, 500 mM NaCl, pH 8.0), LDPE film (2 \times 1 cm, ca. 40 mg), and GPx (1 mg/mL). Reaction buffer supplemented with the LDPE film was used as the control group. All treatments were incubated at 30 °C for 96 h and performed in triplicate. Then, residual LDPE films were recovered and rinsed with ddH₂O. After dried at 30 °C, LDPE films were weighed to determine the weight loss as previously described. Subsequently, molecular weight analysis (HT-GPC), surface morphology observation (SEM and AFM), hydrophobicity assessment (WCA), tensile strength testing, and functional group characterization (FTIR) were conducted on the LDPE sample, following the methods described above. GC-MS was used to detect the biodegradation products released from the LDPE film by GPx. Briefly, the solution after the reaction was air-dried using nitrogen gas, and the precipitate was redissolved in 1 mL solvent mixed by dichloromethane and methanol (1:1). The redissolved sample was centrifuged to collect the supernatant at 6000 rpm and 4 $^{\circ}\text{C}$ for 30 min. Then, 10 μL supernatant was used for GC-MS analysis as aforementioned method.

2.8.6. Superoxide radical anion analysis

Lucigenin (SS0112, Fount Beijing Bio-Tech Co., LTD) was used as a superoxide anion radical (O_2^{\bullet}) indicator during the degradation of LDPE by GPx (Zadjelovic et al., 2022). A 4 mM working solution of lucigenin was prepared by dissolving it in dimethyl sulfoxide. First, the enzymatic degradation of GPx with LDPE was conducted within the buffer of GPx (20 mM Tris-HCl, 500 mM NaCl, pH 8.0). Four experimental groups were designed: (1) buffer (4 mL); (2) buffer (4 mL) + LDPE (2 × 1 cm, ca. 40 mg); (3) GPx (1 mg/mL, 4 mL); (4) GPx (1 mg/mL, 4 mL) + LDPE (2

 \times 1 cm, ca. 40 mg). Each experimental group was performed in 12 replicates and incubated at 30 °C for 96 h. The reaction mixture from three replicates of each group was collected every 24 h and centrifuged at 12,000 rpm for 1 min. Then, 1 mL supernatant was added with 1% lucigenin (v/v) working solution and reacted for 30 min at 30 °C under the dark condition. To measure the fluorescence, 200 μL of supernatant was taken from each sample and placed in a black 96-well plate. The lucigenin oxidized by $O_2^{-\bullet}$ was measured using a fluorescence spectrometer (FlexStation3, Molecular Devices) at 390/440 nm λ_{ex} / λ_{em} .

3. Results

3.1. Enrichment and isolation of a marine bacterium that degrades PE powder

Surface seawater and sediment samples were obtained from 57 stations in the Changjiang Estuary and East China Sea; the information of these sampling stations is shown in Table S2. All samples were inoculated and cultured in CFM with PE powders (Mn: 1700 and Mw: 4000) as sole carbon source, and only the seawater sample from B6 station in the Changjiang Estuary showed obvious microbial growth in three culture stages (30 days for each stage) (Fig. S3). As enrichment progressed, the

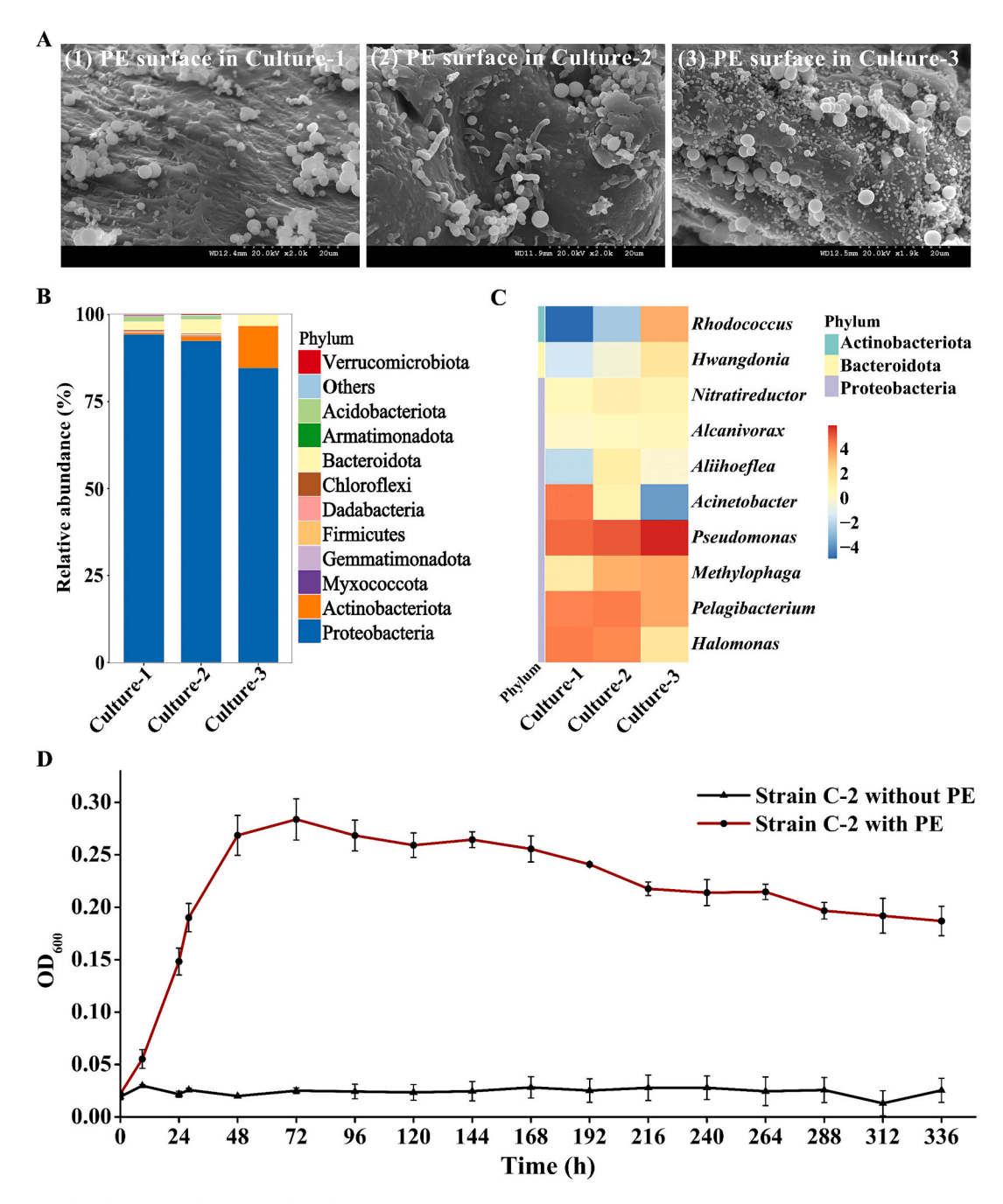


Fig. 1. Enrichment and isolation procedures of PE-degrading strain C-2.

A, SEM observation of colonization by microbiota and morphological change of PE powders in primary culture (Culture-1), secondary culture (Culture-2) and tertiary culture (Culture-3). B, Microbiota composition in three culture stages at the phylum level. C, Heatmap of species relative abundance in three culture stages at the genus level. The value of heatmap is normalized by the log₂ transformed relative abundance in row. D, Growth curves of strain C-2 for two-week cultivation in CFM medium with and without PE powders as sole carbon source. The cultivation carried out at 30 °C and 160 rpm.

number of microorganisms attached to the surface of the PE increased substantially, and obvious cracks and pits were observed in the recovered particles (Fig. 1A). We hypothesised that if certain bacteria in the initial sample could degrade PE, their relative abundance will increase significantly during the enrichment process. The results of 16S rRNA gene amplicon sequence analysis indicated a significant increase in the relative abundance of Actinobacteriota bacteria from 0.6% to 12.0% from primary to tertiary cultures (Fig. 1B). Further comparison at the bacterial genus level revealed an enrichment tend of Rhodococcus genus (from 0.03% to 9.55%) of Actinobacteriota (Fig. 1C), and only one Rhodococcus bacterium was identified in the enriched sample based on 16S rRNA amplicon sequence alignment. Therefore, we speculated that the bacterium of Rhodococcus was closely related to the degradation and utilisation of PE powders during the enrichment. To verify this hypothesis, a gram-positive strain designated as Rhodococcus sp. C-2 (GenBank accession number of the 16S rRNA gene: ON078502) was isolated by a ten-fold dilution method from the tertiary culture sample. Then, strain C-2 was cultured in CFM to measure its growth using PE powders as the sole carbon source. The growth curves showed that strain C-2 grew rapidly on PE over two days and maintained steady growth within a week, whereas it failed to grow in the absence of PE carbon source (Fig. 1D). Thus, the above results demonstrate that strain C-2 can utilise low-molecular-weight PE as sole carbon source for individual growth, which led to its competitive advantage in the enrichment

3.2. Verification of strain C-2 as an LDPE-degrading bacterium

According to the HT-GPC test, LDPE film is classified as high molecular weight polyethylene, with a weight average molecular weight (Mw) of 245,991 \pm 1985 and a number average molecular weight (Mn) of 25,411 \pm 327. The purity of LDPE film was determined to be over 99.7% based on the weighing result of the precipitate after dissolution (Table S3). Then, LDPE films were used as carbon sources to evaluate the biodegradability of strain C-2. After 30-day incubation, the control and E. coli treated LDPE films were observed to be smooth and intact (Fig. 2A, B), whereas strain C-2 adhered to the surface of the LDPE film, resulting in cracks and pits around the cells (Fig. 2C). After the removal of surface bacteria, it was observed that the LDPE film treated with strain C-2 had developed cracks and holes, as shown in Fig. S4 and S5. The surface roughness of LDPE treated strain C-2 (124.97 nm) was found to be 5-6 times higher than that of the control group (21.78 nm) and E. coli group (21.98 nm) (Table S4). The contact angle of LDPE treated by strain C-2 decreased 28.95% than control (Table S4), which revealed that the hydrophilicity of the LDPE surface was enhanced following treatment with strain C-2 (Fig. S5F). Moreover, the tensile strength test demonstrated a 9.73% decrease of LDPE after treatment with strain C-2 compared to the tensile strength of control LDPE (Table S4). These alterations in physical properties suggested that strain C-2 had a disruptive effect on the physical structure of LDPE. Besides, the weight of the LDPE film treated with E. coli showed little change compared to that of the control, while the LDPE film treated with strain C-2 showed a significant weight change, and the average weight loss reached 11.23% (Fig. 2D). HT-GPC analysis revealed molecular weight changes in the treated LDPE films (Fig. 2E). Compared with the control group and E. coli group, strain C-2 reduced the Mw and Mn of LDPE films by 28.88% and 21.04%, respectively. Moreover, molecular weight distribution (MWD) curves (Fig. S6) showed depolymerization of the longchain polymer to low-molecular-weight products during the degradation of the LDPE film by strain C-2.

3.3. LDPE biodegradation products released by strain C-2

After degradation by strain C-2, the residual LDPE films were analyzed using ATR-FTIR, and the released products from LDPE were characterized by GC-MS analysis. ATR-FTIR spectroscopic analysis was

used to detect the functional groups in residual LDPE films over 30 days. The basic absorption peaks in the IR spectra indicate the methylene (CH₂) of PE in the vicinity of 2914 cm⁻¹ (asymmetric stretch), 2846 cm⁻¹ 1 (symmetric stretch), 1463 cm⁻¹ (symmetric bend) and 720 cm⁻¹ (rock) (Smith, 2021). Obviously, strain C-2 transformed the chemical groups in the LDPE film, forming significant absorbance peaks at the vicinity of 3370 cm⁻¹, 3090 cm⁻¹, 1720 cm⁻¹, 1650 cm⁻¹ and 1070 cm⁻¹ (Fig. 2F). The functional groups corresponding to these absorption peaks are hydroxyl groups (3550-3200 cm⁻¹), C=C-H bonds $(3100-3000 \text{ cm}^{-1})$, carbonyl groups $(1720-1706 \text{ cm}^{-1})$, C=C bonds (1680-1600 cm⁻¹), and C—O bonds (1150-1050 cm⁻¹), respectively (Albertsson et al., 1987; Peixoto et al., 2017; Watanabe et al., 2009). The presence of these functional groups suggested that hydroxylation and oxidation had occurred during the LDPE degradation process. After treatment with strain C-2, the carbonyl group and double bond indices in LDPE films exhibited a tenfold increase compared to those in the control group (Table S4). Additionally, the increase in double bond index exhibited a significantly greater magnitude compared to that of the carbonyl index, underscoring the paramount importance of C=C bond formation during LDPE biodegradation.

To assess the products of the LDPE film released into the medium, the liquid culture was analyzed using GC–MS after 30-day degradation. By comparing the significant different peaks (intensity $>10^8$) between LDPE-added and glucose-added groups on the chromatogram, seven potential degradation products were identified in the experimental sample (Fig. 2G). Based on the mass spectra of each compound matching in the NIST library (match score > 800), the detected compounds were identified as 1-hexadecanol ($C_{16}H_{34}O$), 1-octadecene ($C_{18}H_{36}$), 1-heneicosyl formate ($C_{22}H_{44}O_2$), 10-octadecenoic acid methyl ester ($C_{19}H_{36}O_2$), 1-nonadecanol ($C_{19}H_{40}O$), 2-methyl-1-hexadecanol ($C_{17}H_{36}O$) and 17-pentatriacontene ($C_{35}H_{70}$), respectively (Fig. S7). GC–MS results demonstrated that multiple products such as short-chain alkenes, alcohol, esters and aldehydes were released from LDPE by the degradation of strain C-2.

3.4. Genomic and transcriptomic analyses of strain C-2

The assembled genome of strain C-2 consisted of 7,039,419 bp with 99.94% completeness and 57.31% GC content. Phylogenetic analysis reconstructed a maximum-likelihood phylogenomic tree with the best substitution model (LG + F + R5) based on 1308 concatenated protein sequences from 19 genome sequences of *Rhodococcus* from the NCBI database (Fig. S8). The genome sequence of strain C-2 shared an average nucleotide identity (98.55%) with R. qingshengii (GCA_019279115.1), clarifying its genetic relationship. Genome annotation predicted 6700 protein-coding genes with functions (Supplementary Data 1), including alkane monooxygenases and peroxidases potentially involved in PE degradation, based on previous reports (Gao et al., 2022; Yoon et al., 2012). Unfortunately, laccase, manganese peroxidase and lignin peroxidase genes were not found in the genome of strain C-2.

To further identify potential PEases in strain C-2, transcriptomic analysis was performed by incubation of strain C-2 in LCM medium supplemented with or without LDPE films. The control group relied only on the growth of low-carbon sources in the LCM medium to better distinguish the metabolic activity of PE degradation from that of general carbon sources. Based on the growth curve of strain C-2 (Fig. S9), a timepoint of 30 days was selected for sequencing, considering the substantial degradation of LDPE film by this strain at depletion of additional carbon sources. According to the differentially expressed gene analysis, 528 genes with significantly (P value \leq 0.05) upregulated (log₂FC > 0.5) expression levels were screened in the experimental group compared to the control group (Fig. 3A). With reference to the gene function annotation of the strain C-2 genome (Supplementary Data 2), the upregulated genes encoded 244 hypothetical proteins and 284 predicted functional proteins. Furthermore, the upregulated genes coding for functional proteins (Supplementary Data 2) participated in the process of transport

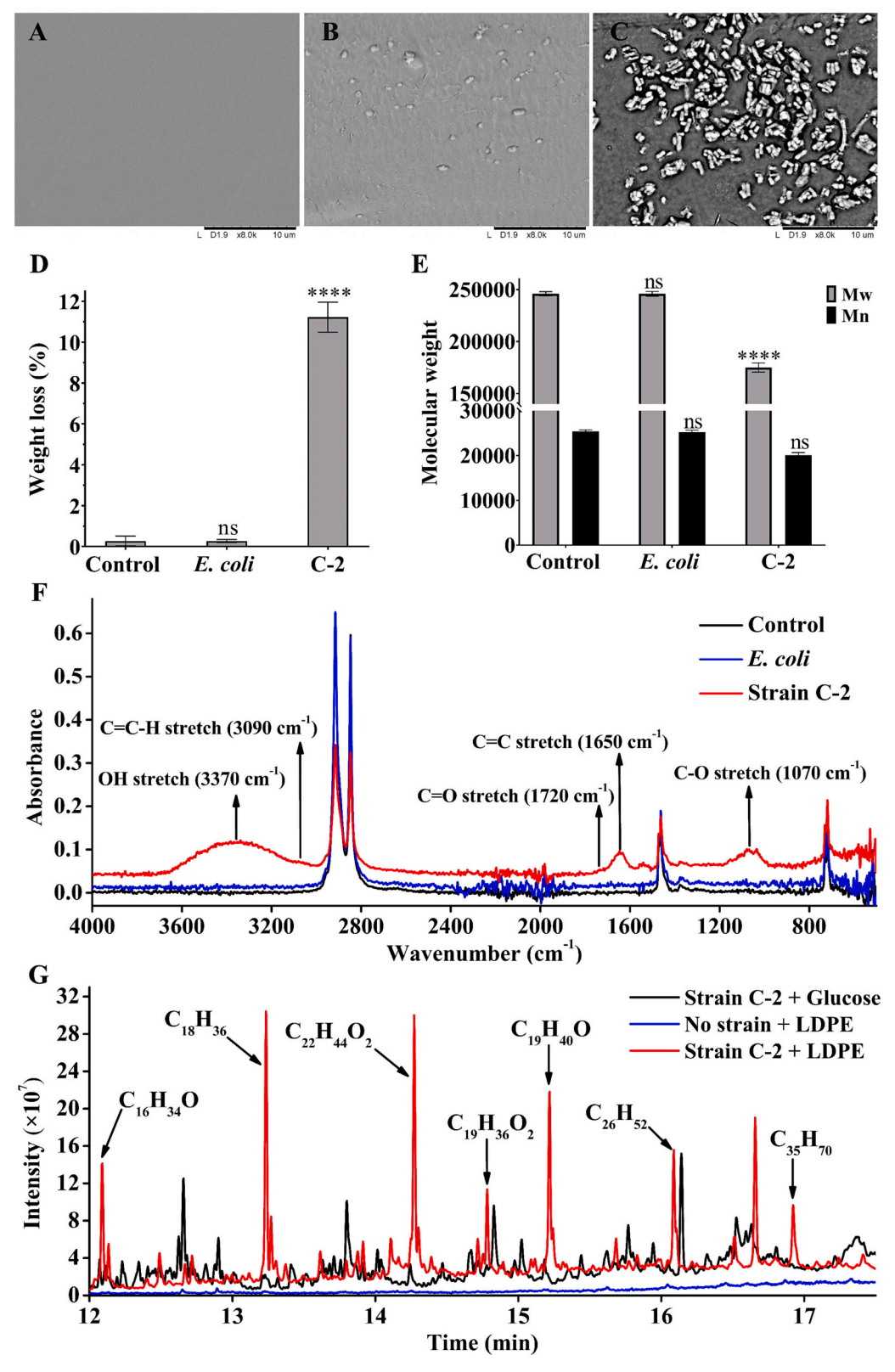


Fig. 2. Physicochemical characterization of LDPE film degradation by strain C-2. A–C, The scanning electron micrographs of control LDPE film (A), surface bacterial adhesion and morphology of LDPE film incubated with E. coli (B), strain C-2 (C) were observed at magnification of 8000, respectively. D, The weight loss of treated LDPE films (strain C-2 or E. coli added) versus control (no strain) after 30 days of experiment. E, Molecular weight (Mn and Mw) reduction of treated LDPE films (strain C-2 or E. coli added) versus control (no strain) after 30 days of experiment. All values represent mean \pm standard deviation (n=3). Significance (Student's t-tests, Dunnett's multiple comparisons test) p < 0.0001 indicated by ****, no statistical significance indicated by ns. F, ATR-FTIR spectra analysis of control (no strain) and bacterial treated (E. coli or strain C-2) LDPE film after 30-day incubation. Functional groups are indicated by upward arrows. G, The GC–MS analysis and comparison of degradation products from strain C-2 incubated in CFM medium with LDPE film or glucose (Glu). No strain inoculated into CFM medium containing LDPE and Glu was used as blank control. LDPE degradation products are indicated by a downward arrow.

(51 genes, e.g., ABC transporter and permease protein), cell growth and energy metabolism (189 genes, e.g., transcriptional regulator, glutamate synthase and succinate dehydrogenase), and xenobiotic degradation (44 genes, e.g., steroid delta-isomerase, chlorocatechol 1,2-dioxygenase and peroxidase) based on GO enrichment (Fig. S10), and KEGG pathway analyses (Fig. S11). According to the reported enzymes related to PE and alkane degradation (Ji et al., 2013; Restrepo-Flórez et al., 2014), 16 bacterial enzymes were screened from 44 xenobiotic degradation proteins, including four peroxidases, six monooxygenases, two lipases, two carboxylesterases, and two dehydrogenases (Fig. 3B). Here, a number of peroxidases and monooxygenases could participate in the depolymerization of polymers, and other enzymes such as lipases might catalyse the further degradation of oligomer products.

3.5. A glutathione peroxidase involved in LDPE depolymerization

Notably, among the highly expressed enzymes, only peroxidases have been reported to individually depolymerize high-molecular-weight polyethylene polymers (Ehara et al., 2000; Gao et al., 2022), potentially playing a key role in the LDPE degradation process mediated by strain C-2. In the differential expressed gene analysis, glutathione peroxidase (GPx) was the most upregulated among different peroxidases so that it required further investigation (Fig. 3B). In the quantitative reverse transcription PCR analysis, the relative abundance of GPx was significantly upregulated (log₂FC > 0.5) during LDPE degradation by strain C-2 (Supplementary Data 3), which was consistent with the results of the transcriptomic analysis. These results indicated that GPx was motivated by LDPE degradation in strain C-2 and participated in the degradation process.

The sequence comparison of GPx with proteins in UniProtKB database found the closest glutathione peroxidase-like protein GPX-2 (accession number: P73824.1) with 53.90% amino acid sequence identity, which derived from *Synechocystis* PCC 6803 and had the ability to reduce fatty acid hydroperoxides or alkyl hydroperoxides (Gaber et al., 2004). Ten protein sequences with the highest identity (45%–54%) were selected for multiple sequence alignment with GPx, and this result indicated significant conserved amino acid sites (Fig. S12A). According to the typical structural and biochemical results of glutathione peroxidase (Zhang et al., 2008), the catalytic traid of GPx would be composed of Cys37, Gln71 and Trp125. The structure predicted by

AlphaFold2 showed that GPx could be a monomeric protein consisting of four β -strands clustered as the central β -sheet surrounded by five α -helices, and two 3_{10} -helices (η -helices) as well as a β -hairpin involving two β -strands (Fig. S12B). The characteristic catalytic site was located on the protein surface, leading to the exposed state of substrate binding region (Fig. S12C).

To characterize the PE degradation activity in vitro, the GPx gene was transformed into E. coli BL21 (DE3) cells for expression and purification. According to the predicted pI of 4.43, the purification process was conducted at pH 8.0, resulting in the successful isolation of a pure protein band with a molecular weight of approximately 18 kD, which closely matched the theoretical Mw of GPx (17.6 kD) (Fig. S13). The purified protein GPx exhibited glutathione catalase activity (76 U/mg) as determined by enzyme analysis. Moreover, GPx also reacted with LDPE film at 30 °C for 96 h. SEM and AFM images showed small cracks and pits on the surface of LDPE film treated by GPx compared with the control (Figs. 4A, B and S14). Compared to the control group, the surface roughness of LDPE treated with GPx exhibited an approximately fourfold increase (Table S6). Additionally, GPx treatment resulted in a 20.24% reduction in water contact angle and a 9.66% decrease in tensile strength of LDPE film (Table S6). After weighing, it was found that the addition of GPx significantly reduced the weight of LDPE by 5.33%. Furthermore, HT-GPC analysis revealed the MWD, reflecting a decrease in high molecular weight polymers and an increase in low molecular weight products (Fig. 4C). At the same time, the molecular weight of LDPE treated with GPx (Mw = 170,292, Mn = 9653) was 30.2% lower than that of the control group (Mw = 243,906, Mn = 14,990) (Fig. 4D). Together, they indicated the depolymerization of the LDPE films. The FTIR analysis revealed functional groups including hydroxyl groups, carbonyl groups, C=C bonds and C-O bonds in the LDPE film treated with GPx (Fig. 4E). The increase in IDBI observed in the carbonyl group and double bond index was found to be statistically significant (Table S7), suggesting that the primary product of LDPE degradation catalyzed by GPx was the formation of carbon-carbon double bonds. This finding was consistent with previous results obtained from LDPE treated by strain C-2, thereby highlighting the significance of GPx in the biodegradation process of LDPE by strain C-2. Based on the GC-MS results, four potential degradation products were identified by comparing the peaks with significant differences between the experimental and control groups (Fig. 4F): 1-dodecene (C12H24), n-hexadecanoic acid

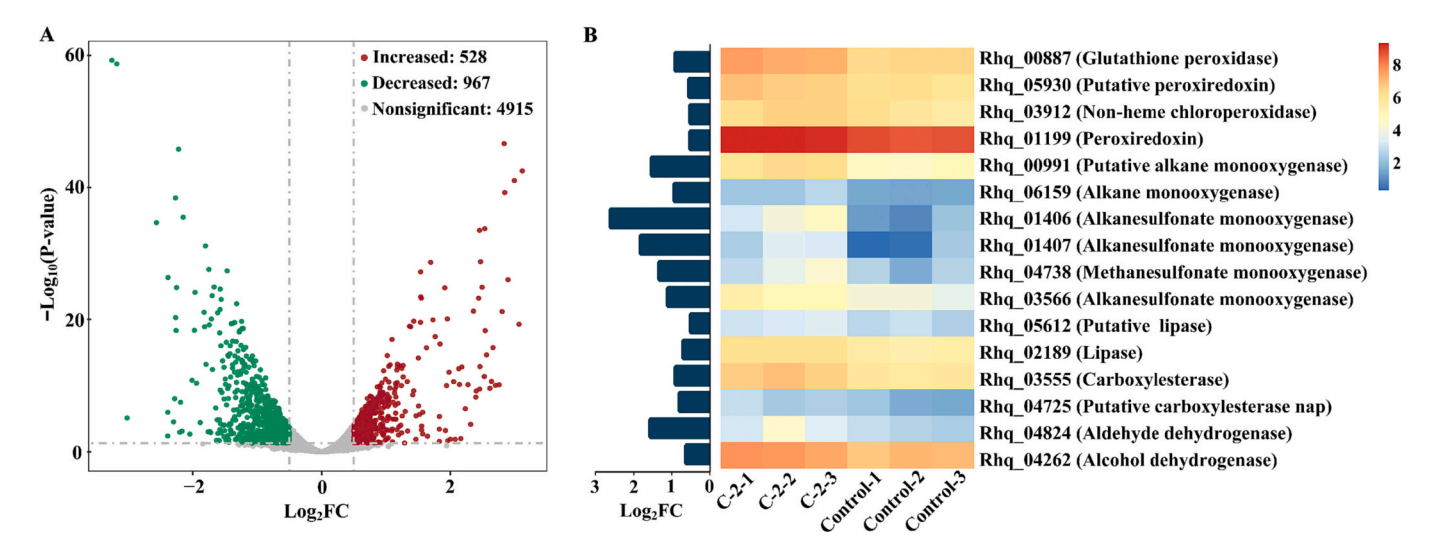


Fig. 3. Transcriptomic analysis of LDPE-degradation by strain C-2.

A, Volcano map showing protein-coding genes that were significantly increased (red spheres) and decreased (green spheres) in the expression level of the experimental group compared with the control group. All differential genes in two groups were identified by the quasi-likelihood F test and nonsignificant results (gray spheres) represent nondifferential genes. B, 16 enzymes participating in the degradation metabolism of LDPE film. The bar graph showed the up-regulated levels of 16 enzymes based on the log₂ transformed values of fold change. The heatmap displayed the expression level of 16 enzymes using corresponding FPKM normalized by log₂ transformed counts in the control and experimental groups.

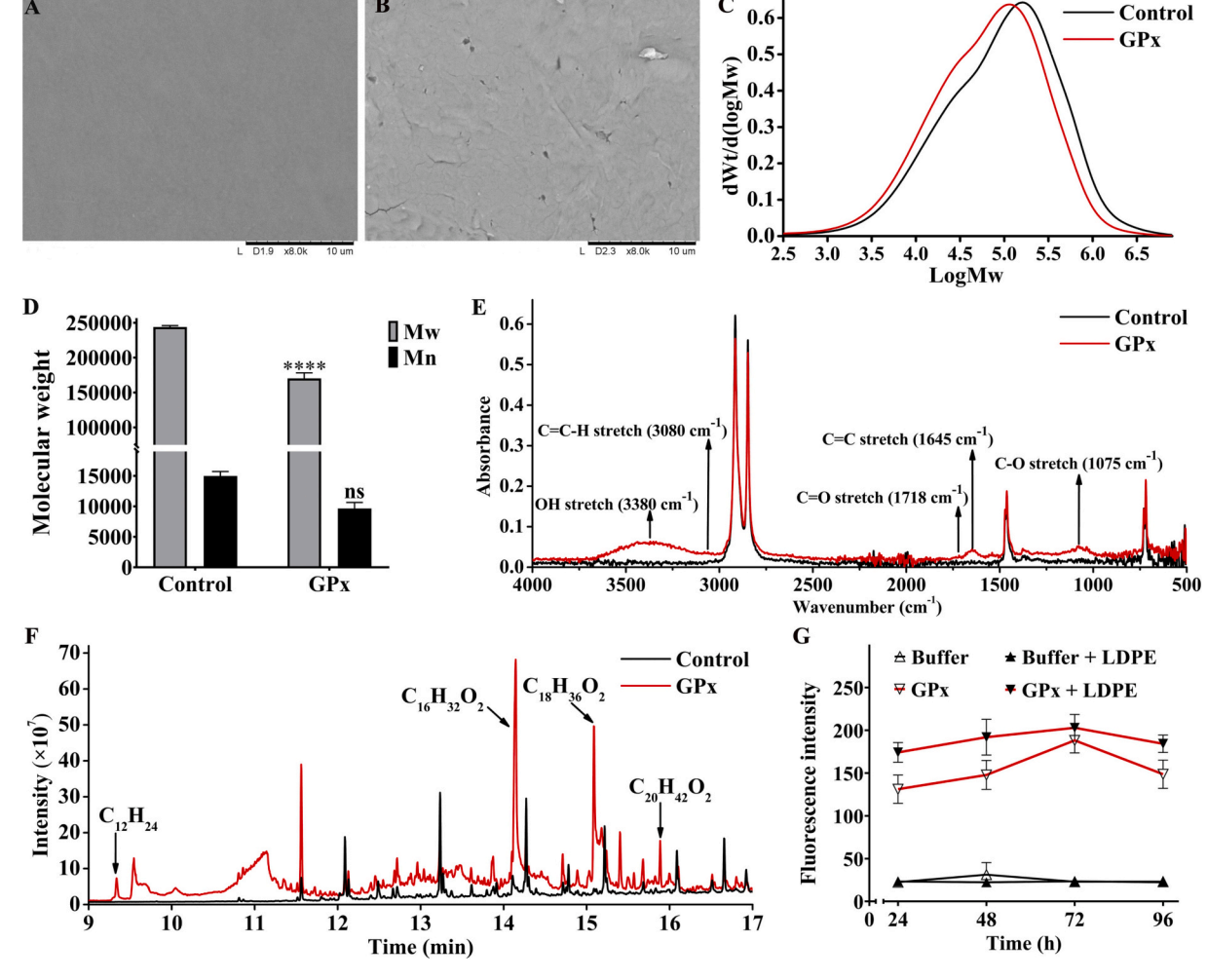


Fig. 4. Physicochemical characterization of LDPE degradation by glutathione peroxidase (GPx).

A, SEM observation of the LDPE film treated by protein buffer for 96 h (control). B, SEM observation of the LDPE film treated by 1 mg/mL GPx for 96 h. C, Molecular weight distribution (MWD) of LDPE films treated by protein buffer (control) and GPx (1 mg/mL). D, Molecular weight of LDPE films treated by protein buffer (control) and GPx (1 mg/mL). Infrared spectroscopy measures absorption peaks in the wavenumer of 4000–500 cm⁻¹. Functional groups are indicated by upward arrows. F, GC–MS analysis of products released from the LDPE film treated by 1 mg/mL GPx and protein buffer (control). The different peak intensity of same retention time in the experimental group and the control group is considered as potential degradation product for mass spectrum analysis. Degradation products are indicated by a downward arrow. G, The fluorescence intensity reflecting the superoxide radical anion production change within 96 h during the degradation of LDPE by enzyme GPx.

 $(C_{16}H_{36}O_2)$, octadecanoic acid $(C_{18}H_{36}O_2)$, and 2-(octadecyloxy) ethanol $(C_{20}H_{42}O_2)$ (Fig. S15). The chemical bonds in these alkenes, carboxylic acids and alkanol products corresponded precisely to the emerging functional groups in the residual LDPE. This evidence indicates that GPx depolymerize LDPE by cleaving long carbon chains via multi-step reactions such as hydroxylation and oxidation, generating hydrophilic groups as well as releasing short-chain products.

To verify whether superoxide anion radical (O_2^{\bullet}) is involved in the degradation of GPx towards LDPE, the change of O_2^{\bullet} during the process of enzymatic degradation was measured based on fluorescence reaction (Fig. 4G). Weak fluorescence intensity indicated that buffer and LDPE hardly produce O_2^{\bullet} under degradation reaction conditions. Interestingly, the peroxidase GPx can gradually produce O_2^{\bullet} , and reached a peak in approximately 72 h. Then, the radical began to decline possibly due to enzyme inactivation. While GPx reacted with LDPE, the GPx and LDPE group produced relatively more O_2^{\bullet} than the GPx group, which elucidated that this radical was released by GPx and involved in the enzymatic degradation of LDPE.

4. Discussion

Abundant plastic debris and microplastics have been discovered in the surface water and sediments of the Changjiang Estuary and East China Sea, and PE plastics are statistically dominant in water samples obtained from these areas (Peng et al., 2017; Xu et al., 2018; Zhang et al., 2019; Zhao et al., 2019). Therefore, samples from this area were used to isolate PE degrading bacteria. During the multi-stage enrichment of water samples obtained from the Changjiang Estuary, the relative abundance of Rhodococcus genus showed a sharp upward trend in the medium with PE as the sole carbon source, and a strain of Rhodococcus designated as strain C-2 was successfully isolated to degrade LDPE. There have been previous reports of Rhodococcus bacteria degrading polyethylene, such as *Rhodococcus opacus* R7 (Zampolli et al., 2021) and Rhodococcus ruber C208 (Gilan (Orr) et al., 2004). Strain C-2 is the closest genetic relative to R. qingshengii (ANI > 95%) and is firstly described as a PE degrading bacterium. Here, we define the PE degradation efficiency as the average weight loss per day, and strain C-2 shows a stronger LDPE degradation ability than the other reported bacteria, such as Bacillus, Alcanivorax as well as other Rhodococcus bacteria (Table 1). Considering the resistance to various stress conditions (e.g., stress due to metals and organic solvents) of Rhodococcus (Cappelletti et al., 2020), strain C-2 may be considered as a plastic degrader for plastic waste treatment in situ. According to enzymatic experiments in vitro, the enzymes that play a key role in the degradation of polyethylene mainly include laccases (Zhang et al., 2022) and peroxidases (Gao et al., 2022). In comparison to different PEases in previous research, their degradation efficiency is usually measured by the molecular weight reduction. In this study, GPx demonstrates a remarkable depolymerization effect on LDPE film, surpassing the activity of glutathione peroxidase in marine fungi Alternaria alternata FB1 by 18% (Gao et al., 2022) and laccase in actinomycete Rhodococcus ruber by 20% (Santo et al., 2013). In addition, the degradation of PE film by laccase in Rhyzopertha Dominica resulted in a 12.94% reduction in the surface contact angle (Zhang et al., 2022), which was comparatively lower than the 20.24% decrease observed for LDPE film treated with GPx. The current state of research suggests that GPx exhibits the highest efficacy as an enzyme for the degradation of LDPE film. Therefore, this study provides a low-cost and eco-friendly biological agent for tackling plastic pollution.

Currently, the molecular mechanism of of enzyme-catalyzed polyethylene depolymerization is still unclear. In fact, inert C—C bonds and long chain structure hinder the reaction between LDPE and most enzymes so that long carbon chain polymer may only be depolymerized by high-energy redox reactions (Inderthal et al., 2021; Yao, Z. et al., 2022). Therefore, we hypothesised that PEase evolved from existing enzymes that possess strong redox properties, such as glutathione peroxidase, and evolved PEases could catalyse the depolymerization of polymers based on exposed catalytic active sites. In the present study, we first verify that the glutathione peroxidase GPx derived from strain C-2 can depolymerize LDPE in vitro, and the predicted three-dimensional structure also discloses a catalytic triad (Cys37-Gln71-Trp128) in the surface of GPx. This characteristic exposure of active site facilitates the enzyme's attack on the polymer substrate, which is present in evolving esterase structure that degrades poly(ethylene terephthalate) plastic (Joo et al., 2018). In

addition, fluorescence experiments show that GPx can release superoxide anion radical when reacting with LDPE, which may be related to the covalent lysine-cysteine redox switch (NOS redox bridge) in the internal structure of enzyme (Wensien et al., 2021). In fact, NOS redox bridge is widespread in oxidoreductases combined with oxygen, and this redox switch reversibly altered the oxidized or reduced state of the enzyme as a protein structure allosteric switch to prevent the overoxidation of crucial cysteine residues (Rabe von Pappenheim et al., 2022). Thus, an NOS redox bridge in GPx may be formed by Cys with adjacent Lys, which binds to oxygen or O2 • to protect proteins from overoxidation damage under oxidative stress. In contrast, disengagement of the NOS redox bridge between Cys and Lys switches GPx to a reduced state with the formation of superoxide radical anion, which facilitates peroxidase to catalyse substrates. Based on this redox switch and hydrocarbon oxidation mechanism by superoxide anions (Frimer et al., 1986), a putative depolymerization pathway is driven by the collaboration between GPx and its releasing superoxide anions (Fig. 5). At the initial depolymerization, $O_2^{-\bullet}$ dissociated from GPx activates the long carbon chain by attacking C—H bonds to abstract hydrogen atoms from the methylene. The resulting carbon-based radicals may partly form C=C bonds with adjacent carbon free radicals. Then, molecular oxygen is involved in the oxidation of the carbon chain, which produces peroxy intermediates (ROO.). On the one hand, ROO. is again attacked by O2. to form a carboxyl group (Frimer et al., 1986). On the other hand, ROO can then continue to abstract hydrogen atoms from nearby carbon chains to form hydroperoxides (R-O···H) and new free radicals (R*), triggering a chain reaction (Albertsson et al., 1987). Subsequently, GPx reduces the hydroperoxides to hydroxyl groups, which are unstable when attached to C=C bonds and may break the double bond to form carbonyl groups. In conclusion, GPx triggers the initial cleavage of C-C bonds and C-H bonds in the polymer, leading to the physical structure destruction of LDPE and the release of short-chain products (e.g., alkene and alkanol) from LDPE films. Accordingly, our findings contribute to the understanding of LDPE degradation pathway.

Based on the genomic, transcriptomic, and biodegradation product

Table 1Identified bacterial strains with the ability to degrade LDPE films.

Strains	Isolation source	Degradable polymer type	Degradation time (days)	Weight loss (%)	Degradation efficiency (%/d)	Reference
Rhodococcus sp. C-2	Sea water	LDPE film	30	11.23	0.37	This study
Bacillus sphericus	Shallow water	LDPE film	365	10.00	0.03	(Sudhakar et al., 2008)
Kocuria palustris M16	Coastal water	LDPE bag	30	1.00	0.03	(Harshvardhan and Jha, 2013)
Bacillus pumilus M27	Coastal water	LDPE bag	30	1.50	0.05	(Harshvardhan and Jha, 2013)
Bacillus subtilis H1584	Coastal water	LDPE bag	30	1.75	0.06	(Harshvardhan and Jha, 2013)
Bacillus sp. AIIW2	Coastal water	LDPE film	90	0.96	0.01	(Kumari et al., 2019)
Cobetia sp. H237	Ocean	LDPE film	90	1.40	0.02	(Khandare et al., 2021)
Halomonas sp. H255	Ocean	LDPE film	90	1.72	0.02	(Khandare et al., 2021)
Exigobacterium sp. H256	Ocean	LDPE film	90	1.26	0.01	(Khandare et al., 2021)
Alcanivorax sp. H265	Ocean	LDPE film	90	0.97	0.01	(Khandare et al., 2021)
Enterobacter asburiae YT1	Waxworm gut	LDPE film	60	6.10	0.02	(Yang et al., 2014)
Bacillus sp. YP1	Waxworm gut	LDPE film	60	10.70	0.18	(Yang et al., 2014)
Serratia sp.	Plastic debris	LDPE pieces	150	40.00	0.27	(Nadeem et al., 2021)
Stenotrophomonas sp.	Plastic debris	LDPE pieces	150	32.00	0.21	(Nadeem et al., 2021)
Pseudomonas sp.	Plastic debris	LDPE pieces	150	21.00	0.14	(Nadeem et al., 2021)
Paenibacillus sp.	Landfill soil	LDPE film	90	11.60	0.13	(Bardají et al., 2019)
Rhodococcus ruber	Landfill soil	LDPE film	30	8.00	0.27	(Gilan (Orr) et al., 2004)
Brevibacillus borstelensis	Landfill soil	LDPE film	30	2.50	0.08	(Hadad et al., 2005)
Bacillus siamensis	Landfill soil	LDPE film	90	8.46	0.09	(Maroof et al., 2021)
Bacillus wiedmannii	Landfill soil	LDPE film	90	5.39	0.06	(Maroof et al., 2021)
Bacillus cereus	Landfill soil	LDPE film	90	6.33	0.07	(Maroof et al., 2021)
Pseudomonas aeruginosa	Landfill soil	LDPE film	90	1.15	0.01	(Maroof et al., 2021)
Acinetobacter iwoffii	Landfill soil	LDPE film	90	0.76	0.01	(Maroof et al., 2021)
Bacillus sp. PE3	Landfill soil	LDPE film	30	6.68	0.22	(Kavitha and Bhuvaneswari, 2021)
Bacillus amyloliquefaciens BSM-2	Landfill waste	LDPE film	60	14.70	0.25	(Das and Kumar, 2015)

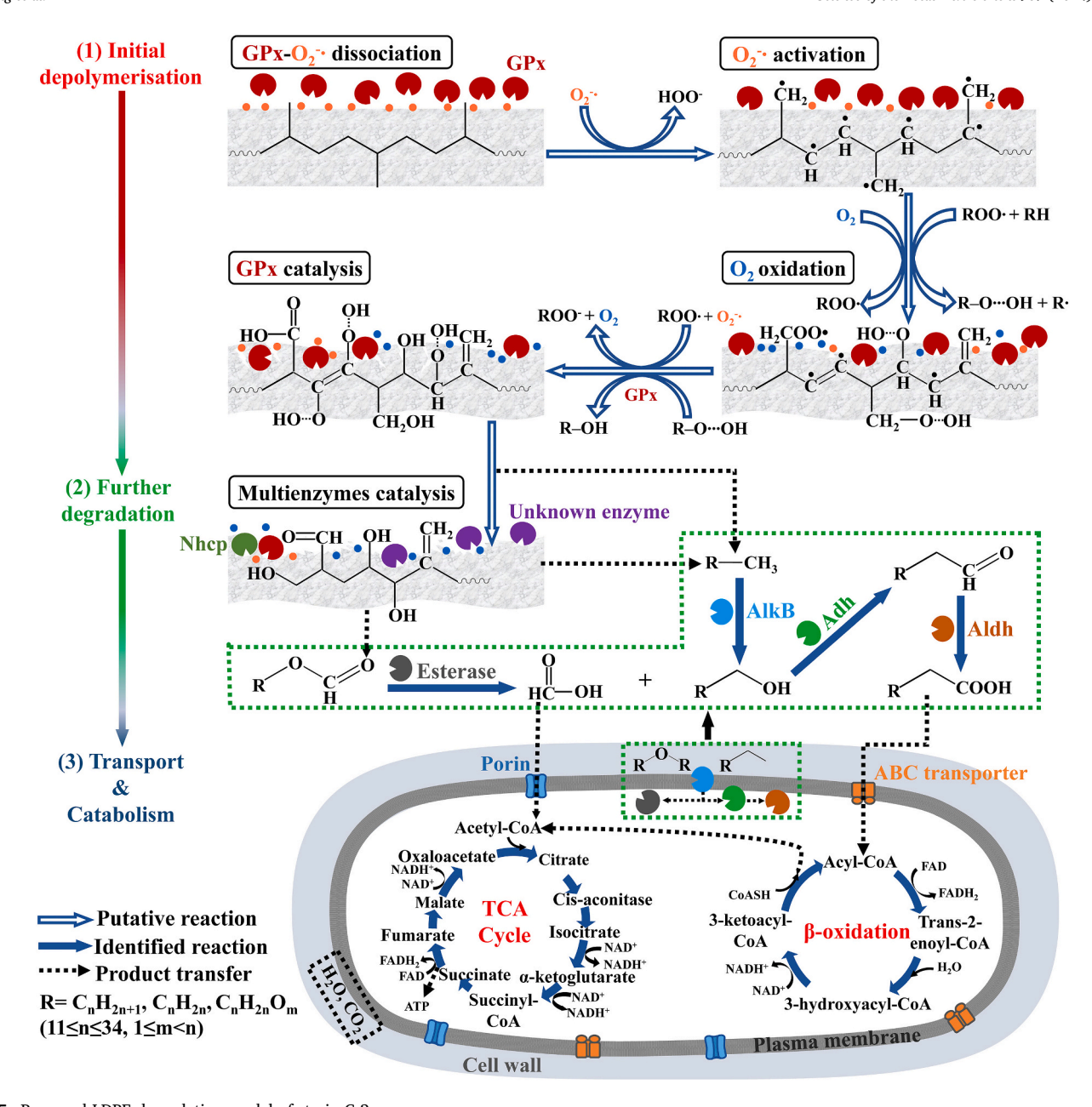


Fig. 5. Proposed LDPE degradation model of strain C-2. The pathway was proposed by combining the analysis of genomic, transcriptomic and product results of strain C-2 during the growth with LDPE film, which is mainly divided into three stages, including initial depolymerization, further degradation and intracellular assimilation. In the initial depolymerization, the superoxide anion radical (O_2^{\bullet}) dissociated from the glutathione peroxidase (GPx) activates LDPE, and GPx then catalyses the chain scission of LDPE with oxygen. In the further degradation, non-heme chloroperoxidase (Nhcp) and unknown enzyme successively break polymer chain to release shorter chain products $(12 \le C \le 35)$, which are further oxidized by membrane-spanning alkane hydroxylase (AlkB), alcohol dehydrogenase (Adh) and aldehyde dehydrogenase (Aldh) (Framed in green box). The short-chain fatty acids bind to ABC transporters or pass the porin protein and enter the cell. Finally, the fatty acid products consecutively undergo β -oxidation and other enzymes are predicted to be involved in LDPE degradation in transcriptome and genome results. Blue circles represent by oxygen, and orange circles represent superoxide anion radicals. Solid arrows represent the identified reactions while hollow arrows represent the putative reactions, and dashed arrows indicate the

analyses, the LDPE degradation model would include initiatial depolymerization of GPx, further degradation by multienzyme catalysis, as well as transport and intracellular catabolism of short chain products (Fig. 5). In the initial depolymerization, the glutathione peroxidase GPx activates the LDPE backbone by dissociating the superoxide anion radicals. Under the catalysis of GPx and free radicals, C—C bonds and C—H bonds in LDPE are splitted to form oxygen-containing functional groups such as hydroxyl groups and carbonyl groups. In this process, chain scission occurs in long-chain polymers, and some short-chain products

transfer of products.

(C12–C20) including alkenes, carboxylic acid and alkanols are released into the environment, resulting in morphological changes on the surface of LDPE (Fig. 4). Compared with the degradation products of LDPE by strain C-2 such as esters and aldehydes (Fig. 2G), it is speculated that multiple enzymes participate in the further degradation of depolymerized LDPE. Heme and non-heme iron-dependent enzymes, particularly chloroperoxidases, can readily activate oxygen and oxidatively cleave C—C bonds to generate corresponding carbonyls, such as ketones and aldehydes (Huang et al., 2021; Mutti, 2012). In consequence, the

highly expressed non-heme chloroperoxidase (Fig. 3B) might further oxidise the C=C bonds in the depolymerized LDPE to form carbonyl groups. When the carbon atom numbers in the hydrocarbon products are reduced to a certain number (12 \leq carbon atoms (C) \leq 35 found in this study, Fig. 4E), it can be further oxidized by alkane hydroxylase on the plasma membrane (Guo et al., 2023). Alkane monooxygenases have been reported to degrade low-molecular-weight polyethylene (1700–23,700) via terminal and terminal oxidation (Restrepo-Flórez et al., 2014; Yoon et al., 2012). Therefore, short-chain products can be hydroxylated by alkane monooxygenase to form alkanols, which are then sequentially converted to carboxylic acids by alcohol dehydrogenase and aldehyde dehydrogenase. In addtion, ester products can be hydrolyzed carboxylic acids and alcohols by esterase or lipase (Ji et al., 2013). After the catalysis of multiple enzymes, fatty acids with different chain lengths are transported into the cell through the transport system on plasma membrane. Briefly, long-chain fatty acids (C \geq 12) are probably transported into the cell by fatty acid ABC transporters, whereas short-chain fatty acids (C < 11) enter the cell via free diffusion or porins (Heinkel et al., 2018; Jimenez-Diaz et al., 2017). Finally, fatty acids taken up by cells enter the β-oxidation pathway to produce acetyl-CoA, which is subsequently converted into energy in the tricarboxylic acid cycle to support cell growth.

5. Conclusion

In the present study, an LDPE-degrading strain C-2, which is genomically closest to Rhodococcus qingshengii, was successfully enriched and isolated as a pure culture from water samples obtained from the Changjiang Estuary. SEM analysis indicated that strain C-2 grew on plastic surface and destroyed the structure of the LDPE film. The weight loss and HT-GPC results confirmed the high degradation capability and efficiency of strain C-2 towards LDPE films. Together with the ATR-FTIR and GC-MS analyses, strain C-2 split the long carbon chain of LDPE via hydroxylation and oxidation, forming hydrophilic functional groups and releasing short-chain products. Furthermore, genomic and transcriptomic analyses disclosed multiple enzymes and transporters associated with LDPE degradation such as peroxidases and ABC transporter. A putative degradation pathway in strain C-2 consisting of initial depolymerization, further degradation, products transport and catabolism based on multienzyme collaboration was proposed. Notably, the glutathione peroxidase GPx triggered the initial depolymerization of LDPE as a PEase by releasing superoxide anion radicals and played a key role in LDPE degradation pathway.

Supplementary data to this article can be found online at https://doi.org/10.1016/j.scitotenv.2023.167993.

CRediT authorship contribution statement

Zhen Rong: Collected samples, conducted experiments, data analysis, wrote the manuscript. **Zhi-Hao Ding**: Data analysis. **Yue-Hong Wu**: Designed experiment, edited the manuscript, supervision, Validation. **Xue-Wei Xu**: Conceived experiment, edited the manuscript, supervision, validation.

Declaration of competing interest

The authors declare that they have no known competing financial interests or personal relationships that could have appeared to influence the work reported in this paper.

Data availability

The 16S rRNA gene amplicon sequence data of three culture samples in enrichent process has been deposited in the NCBI database under accession number PRJNA949434. Assembly genome sequence of strain C-2 and raw transcriptomic data during LDPE degradation by strain C-2

have been deposited in the NCBI database under accession number GCA_027854095.1 and PRJNA937200, respectively.

Acknowledgments

This work was supported by National Science and Technology Fundamental Resources Investigation Program of China (2019FY100700). We would like to thank the Shared Voyage Plan (NORC2020-07) established by National Natural Science Foundation of China for sampling support.

References

- Albertsson, A.C., Andersson, S.O., Karlsson, S., 1987. The mechanism of biodegradation of polyethylene. Polym. Degrad. Stab. 18 (1), 73–87. https://doi.org/10.1016/0141-3910(87)90084.X
- Alshehrei, F., 2017. Biodegradation of low density polyethylene by fungi isolated from Red Sea water. Int. J. Curr. Microbiol. App. Sci. 6 (8), 1703–1709. https://doi.org/ 10.20546/jicmas.2017.608.204
- Ameen, F., Moslem, M., Hadi, S., Al-Sabri, A.E., 2015. Biodegradation of low density polyethylene (LDPE) by mangrove fungi from the Red Sea coast. Prog. Rubber Plast. Recycl. Technol. 31 (2), 125–143. https://doi.org/10.1177/147776061503100204.
- Amelia, T.S.M., Khalik, W.M.A.W.M., Ong, M.C., Shao, Y.T., Pan, H.-J., Bhubalan, K., 2021. Marine microplastics as vectors of major ocean pollutants and its hazards to the marine ecosystem and humans. Prog. Earth Planet. Sci. 8 (1) https://doi.org/10.1186/s40645-020-00405-4.
- Andrady, A.L., 1990. Weathering of polyethylene (LDPE) and enhanced photodegradable polyethylene in the marine environment. J. Appl. Polym. Sci. 39 (2), 363–370. https://doi.org/10.1002/app.1990.070390213.
- Andrady, A.L., 2011. Microplastics in the marine environment. Mar. Pollut. Bull. 62 (8), 1596–1605. https://doi.org/10.1016/j.marpolbul.2011.05.030.
- Auta, H.S., Emenike, C.U., Jayanthi, B., Fauziah, S.H., 2018. Growth kinetics and biodeterioration of polypropylene microplastics by *Bacillus* sp. and *Rhodococcus* sp. isolated from mangrove sediment. Mar. Pollut. Bull. 127 (2), 15–21. https://doi.org/ 10.1016/j.marpolbul.2017.11.036.
- Balasubramanian, V., Natarajan, K., Rajeshkannan, V., Perumal, P., 2014. Enhancement of in vitro high-density polyethylene (HDPE) degradation by physical, chemical, and biological treatments. Environ. Sci. Pollut. Res. 21 (21), 12549–12562. https://doi. org/10.1007/s11356-014-3191-2.
- Ballerstedt, H., Tiso, T., Wierckx, N., Wei, R., Averous, L., Bornscheuer, U., O'Connor, K., Floehr, T., Jupke, A., Klankermayer, J., Liu, L., de Lorenzo, V., Narancic, T., Nogales, J., Perrin, R., Pollet, E., Prieto, A., Casey, W., Haarmann, T., Sarbu, A., Schwaneberg, U., Xin, F., Dong, W., Xing, J., Chen, G.Q., Tan, T., Jiang, M., Blank, L. M., 2021. MIXed plastics biodegradation and UPcycling using microbial communities: EU Horizon 2020 project MIX-UP started January 2020. Environ. Sci. Eur. 33 (1), 99. https://doi.org/10.1186/s12302-021-00536-5.
- Bankevich, A., Nurk, S., Antipov, D., Gurevich, A.A., Dvorkin, M., Kulikov, A.S., Lesin, V. M., Nikolenko, S.I., Pham, S., Prjibelski, A.D., Pyshkin, A.V., Sirotkin, A.V., Vyahhi, N., Tesler, G., Alekseyev, M.A., Pevzner, P.A., 2012. SPAdes: a new genome assembly algorithm and its applications to single-cell sequencing. J. Comput. Biol. 19 (5), 455–477. https://doi.org/10.1089/cmb.2012.0021.
- Bardají, D.K.R., Furlan, J.P.R., Stehling, E.G., 2019. Isolation of a polyethylene degrading Paenibacillus sp. from a landfill in Brazil. Arch. Microbiol. 201 (5), 699–704. https://doi.org/10.1007/s00203-019-01637-9.
- Cappelletti, M., Presentato, A., Piacenza, E., Firrincieli, A., Turner, R.J., Zannoni, D., 2020. Biotechnology of *Rhodococcus* for the production of valuable compounds. Appl. Microbiol. Biotechnol. 104 (20), 8567–8594. https://doi.org/10.1007/s00253-020-10861-z.
- Castro Issasi, C.S., Sasaki, M., Quitain, A.T., Kida, T., Taniyama, N., 2019. Removal of impurities from low-density polyethylene using supercritical carbon dioxide extraction. J. Supercrit. Fluids 146, 23–29. https://doi.org/10.1016/j. sunflu.2019.01.003.
- Chamas, A., Moon, H., Zheng, J., Qiu, Y., Tabassum, T., Jang, J.H., Abu-Omar, M., Scott, S.L., Suh, S., 2020. Degradation rates of plastics in the environment. ACS Sustain. Chem. Eng. 8 (9), 3494–3511. https://doi.org/10.1021/ acssuschemeng.9b06635.
- Chen, S., Zhou, Y., Chen, Y., Gu, J., 2018. fastp: an ultra-fast all-in-one FASTQ preprocessor. Bioinformatics 34 (17), i884–i890. https://doi.org/10.1093/ bioinformatics/bty560.
- Danso, D., Chow, J., Streit, W.R., 2019. Plastics: environmental and biotechnological perspectives on microbial degradation. Appl. Environ. Microbiol. 85 (19) https:// doi.org/10.1128/AEM.01095-19.
- Das, M.P., Kumar, S., 2015. An approach to low-density polyethylene biodegradation by Bacillus amyloliquefaciens. 3 Biotech. 5 (1), 81–86. https://doi.org/10.1007/s13205-014-0205-1.
- Dey, A.S., Bose, H., Mohapatra, B., Sar, P., 2020. Biodegradation of unpretreated low-density polyethylene (LDPE) by *Stenotrophomonas* sp. and *Achromobacter* sp., isolated from waste dumpsite and drilling fluid. Front. Microbiol. 11 (12), 603210 https://doi.org/10.3389/fmicb.2020.603210.
- Duffus, J., 1993. Glossary for chemists of terms used in toxicology (IUPAC Recommendations 1993). Pure Appl. Chem. 65 (9), 2003–2122. https://doi.org/ 10.1351/pac199365092003.

- Ehara, K., Iiyoshi, Y., Tsutsumi, Y., Nishida, T., 2000. Polyethylene degradation by manganese peroxidase in the absence of hydrogen peroxide. J. Wood Sci. 46 (2), 180–183. https://doi.org/10.1007/BF00777369.
- Frimer, A.A., Farkash-Solomon, T., Aljadeff, G., 1986. Mechanism of the superoxide anion radical (O2-) mediated oxidation of diarylmethanes. J. Org. Chem. 51 (11), 2093–2098. https://doi.org/10.1021/jo00361a030.
- Gaber, A., Yoshimura, K., Tamoi, M., Takeda, T., Nakano, Y., Shigeoka, S., 2004. Induction and functional analysis of two reduced nicotinamide adenine dinucleotide phosphate-dependent glutathione peroxidase-like proteins in *Synechocystis* PCC 6803 during the progression of oxidative stress. Plant Physiol. 136 (1), 2855–2861. https://doi.org/10.1104/pp.104.044842.
- Galgani, L., Loiselle, S.A., 2021. Plastic pollution impacts on marine carbon biogeochemistry. Environ. Pollut. 268 (Pt A), 115598 https://doi.org/10.1016/j. envpol.2020.115598.
- Galgani, F., Pham, C.K., Claro, F., Consoli, P., 2018. Marine animal forests as useful indicators of entanglement by marine litter. Mar. Pollut. Bull. 135 (8), 735–738. https://doi.org/10.1016/j.marpolbul.2018.08.004.
- Gall, S.C., Thompson, R.C., 2015. The impact of debris on marine life. Mar. Pollut. Bull. 92 (1–2), 170–179. https://doi.org/10.1016/j.marpolbul.2014.12.041.
- Gao, R., Sun, C., 2021. A marine bacterial community capable of degrading poly (ethylene terephthalate) and polyethylene. J. Hazard. Mater. 416, 125928 https://doi.org/10.1016/j.jhazmat.2021.125928.
- Gao, R., Liu, R., Sun, C., 2022. A marine fungus Alternaria alternata FB1 efficiently degrades polyethylene. J. Hazard. Mater. 431, 128617 https://doi.org/10.1016/j ibazmat.2022.128617.
- García-Gómez, J.C., Garrigós, M., Garrigós, J., 2021. Plastic as a vector of dispersion for marine species with invasive potential. A review. Front. Ecol. Evol. 9, 629756 https://doi.org/10.3389/fevo.2021.629756.
- Geyer, R., Jambeck, J.R., Law, K.L., 2017. Production, use, and fate of all plastics ever made. Sci. Adv. 3 (7), e1700782 https://doi.org/10.1126/sciadv.1700782.
- Ghatge, S., Yang, Y., Ahn, J.H., Hur, H.G., 2020. Biodegradation of polyethylene: a brief review. Appl. Biol. Chem. 63 (1) https://doi.org/10.1186/s13765-020-00511-3.
- Gilan (Orr), I., Hadar, Y., Sivan, A., 2004. Colonization, biofilm formation and biodegradation of polyethylene by a strain of *Rhodococcus ruber*. Appl. Microbiol. Biotechnol. 65 (1), 97–104. https://doi.org/10.1007/s00253-004-1584-8.
- Guo, X., Zhang, J., Han, L., Lee, J., Williams, S.C., Forsberg, A., Xu, Y., Austin, R.N., Feng, L., 2023. Structure and mechanism of the alkane-oxidizing enzyme AlkB. Nat. Commun. 14 (1), 2180. https://doi.org/10.1038/s41467-023-37869-z.
- Hadad, D., Geresh, S., Sivan, A., 2005. Biodegradation of polyethylene by the thermophilic bacterium *Brevibacillus borstelensis*. J. Appl. Microbiol. 98 (5), 1093–1100. https://doi.org/10.1111/j.1365-2672.2005.02553.x.
- Harshvardhan, K., Jha, B., 2013. Biodegradation of low-density polyethylene by marine bacteria from pelagic waters, Arabian Sea, India. Mar. Pollut. Bull. 77 (1–2), 100–106. https://doi.org/10.1016/j.marpolbul.2013.10.025.
- Heinkel, F., Shen, L., Richard-Greenblatt, M., Okon, M., Bui, J.M., Gee, C.L., Gay, L.M., Alber, T., Av-Gay, Y., Gsponer, J., McIntosh, L.P., 2018. Biophysical characterization of the tandem FHA domain regulatory module from the *Mycobacterium uberculosis* ABC transporter Rv1747. Structure 26 (7), 972–986. https://doi.org/10.1016/j.
- Huang, Z., Guan, R., Shanmugam, M., Bennett, E.L., Robertson, C.M., Brookfield, A., McInnes, E.J.L., Xiao, J., 2021. Oxidative cleavage of alkenes by O₂ with a non-heme manganese catalyst. J. Am. Chem. Soc. 143 (26), 10005–10013. https://doi.org/ 10.1021/jacs.1005757
- liyoshi, Y., Tsutsumi, Y., Nishida, T., 1998. Polyethylene degradation by lignin-degrading fungi and manganese peroxidase. J. Wood Sci. 44 (3), 222–229. https://doi.org/ 10.1007/BF00521967
- Inderthal, H., Tai, S.L., Harrison, S.T.L., 2021. Non-hydrolyzable plastics—an interdisciplinary look at plastic bio-oxidation. Trends Biotechnol. 39 (1), 12–23. https://doi.org/10.1016/j.tibtech.2020.05.004.
- Jambeck, J.R., Geyer, R., Wilcox, C., Siegler, T.R., Perryman, M., Andrady, A., Narayan, R., Law, K.L., 2015. Plastic waste inputs from land into the ocean. Science 347 (6223), 768–771. https://doi.org/10.1126/science.1260352.
- Jeon, H.J., Kim, M.N., 2013. Isolation of a thermophilic bacterium capable of low-molecular-weight polyethylene degradation. Biodegradation 24 (1), 89–98. https://doi.org/10.1007/s10532-012-9560-y.
- Ji, Y., Mao, G., Wang, Y., Bartlam, M., 2013. Structural insights into diversity and nalkane biodegradation mechanisms of alkane hydroxylases. Front. Microbiol. 4 (58), 1–13. https://doi.org/10.3389/fmicb.2013.00058.
- Jimenez-Diaz, L., Caballero, A., Segura, A., 2017. Pathways for the degradation of fatty acids in bacteria. In: Rojo, F. (Ed.), Aerobic Utilization of Hydrocarbons, Oils and Lipids. Springer International Publishing, Cham, pp. 1–23. https://doi.org/10.1007/ 978-3-319-39782-5 42-1.
- Joo, S., Cho, I.J., Seo, H., Son, H.F., Sagong, H.Y., Shin, T.J., Choi, S.Y., Lee, S.Y., Kim, K. J., 2018. Structural insight into molecular mechanism of poly(ethylene terephthalate) degradation. Nat. Commun. 9 (1), 382. https://doi.org/10.1038/sa1467-018-02881.1
- Jumper, J., Evans, R., Pritzel, A., Green, T., Figurnov, M., Ronneberger, O., Tunyasuvunakool, K., Bates, R., Zidek, A., Potapenko, A., Bridgland, A., Meyer, C., Kohl, S.A.A., Ballard, A.J., Cowie, A., Romera-Paredes, B., Nikolov, S., Jain, R., Adler, J., Back, T., Petersen, S., Reiman, D., Clancy, E., Zielinski, M., Steinegger, M., Pacholska, M., Berghammer, T., Bodenstein, S., Silver, D., Vinyals, O., Senior, A.W., Kavukcuoglu, K., Kohli, P., Hassabis, D., 2021. Highly accurate protein structure prediction with AlphaFold. Nature 596 (7873), 583–589. https://doi.org/10.1038/ s41586-021-03819-2.

- Kavitha, R., Bhuvaneswari, V., 2021. Assessment of polyethylene degradation by biosurfactant producing ligninolytic bacterium. Biodegradation 32 (5), 531–549. https://doi.org/10.1007/s10532-021-09949-8.
- Khandare, S.D., Chaudhary, D.R., Jha, B., 2021. Marine bacterial biodegradation of low-density polyethylene (LDPE) plastic. Biodegradation 32 (2), 127–143. https://doi.org/10.1007/s10532-021-09927-0.
- Kim, M.Y., Kim, C., Moon, J., Heo, J., Jung, S.P., Kim, J.R., 2017. Polymer film-based screening and isolation of polylactic acid (PLA)-degrading microorganisms. J. Microbiol. Biotechnol. 27 (2), 342–349. https://doi.org/10.4014/ imb.1610.10015.
- Kumari, A., Chaudhary, D.R., Jha, B., 2019. Destabilization of polyethylene and polyvinylchloride structure by marine bacterial strain. Environ. Sci. Pollut. Res. 26 (2), 1507–1516. https://doi.org/10.1007/s11356-018-3465-1.
- Law, K.-Y., 2014. Definitions for hydrophilicity, hydrophobicity, and superhydrophobicity: getting the basics right. J. Phys. Chem. Lett. 5 (4), 686–688. https://doi.org/10.1021/jz402762h.
- Letunic, I., Bork, P., 2021. Interactive Tree Of Life (iTOL) v5: an online tool for phylogenetic tree display and annotation. Nucleic Acids Res. 49 (W1), W293–W296. https://doi.org/10.1093/nar/gkab301.
- Li, Z., Wei, R., Gao, M., Ren, Y., Yu, B., Nie, K., Xu, H., Liu, L., 2020. Biodegradation of low-density polyethylene by *Microbulbifer hydrolyticus* IRE-31. J. Environ. Manag. 263, 110402 https://doi.org/10.1016/j.jenvman.2020.110402.
- Maroof, L., Khan, I., Yoo, H.S., Kim, S., Park, H.-T., Ahmad, B., Azam, S., 2021. Identification and characterization of low density polyethylene-degrading bacteria isolated from soils of waste disposal sites. Environ. Eng. Res. 26 (3), 200167 https:// doi.org/10.4491/eer.2020.167.
- Mirdita, M., Schutze, K., Moriwaki, Y., Heo, L., Ovchinnikov, S., Steinegger, M., 2022. ColabFold: making protein folding accessible to all. Nat. Methods 19 (6), 679–682. https://doi.org/10.1038/s41592-022-01488-1.
- Mohanan, N., Montazer, Z., Sharma, P.K., Levin, D.B., 2020. Microbial and enzymatic degradation of synthetic plastics. Front. Microbiol. 11, 580709 https://doi.org/ 10.3389/fmicb.2020.580709.
- Moharir, R.V., Kumar, S., 2019. Challenges associated with plastic waste disposal and allied microbial routes for its effective degradation: a comprehensive review.

 J. Clean. Prod. 208, 65–76. https://doi.org/10.1016/j.jclepro.2018.10.059.
- Montazer, Z., Habibi Najafi, M.B., Levin, D.B., 2019. Microbial degradation of low-density polyethylene and synthesis of polyhydroxyalkanoate polymers. Can. J. Microbiol. 65 (3), 224–234. https://doi.org/10.1139/cim-2018-0335.
- Montazer, Z., Habibi Najafi, M.B., Levin, D.B., 2020. Challenges with verifying microbial degradation of polyethylene. Polymers (Basel) 12 (1). https://doi.org/10.3390/polym12010123
- Mukherjee, S., Kundu, P.P., 2014. Alkaline fungal degradation of oxidized polyethylene in black liquor: studies on the effect of lignin peroxidases and manganese peroxidases. J. Appl. Polym. Sci. 131 (17), 40738. https://doi.org/10.1002/ app.40738.
- Mutti, F.G., 2012. Alkene cleavage catalysed by heme and nonheme enzymes: reaction mechanisms and biocatalytic applications. Bioinorg. Chem. Appl. 2012, 626909 https://doi.org/10.1155/2012/626909.
- Nadeen, H., Alia, K.B., Muneer, F., Rasul, I., Siddique, M.H., Azeem, F., Zubair, M., 2021. Isolation and identification of low-density polyethylene degrading novel bacterial strains. Arch. Microbiol. 203 (9), 5417–5423. https://doi.org/10.1007/s00203-021-02521-1.
- Nagel, B., Dellweg, H., Gierasch, L.M., 1992. Glossary for chemists of terms used in biotechnology (IUPAC Recommendations 1992). Pure Appl. Chem. 64 (1), 143–168. https://doi.org/10.1351/pac199264010143.
- Natarajan, V.P., Zhang, X., Morono, Y., Inagaki, F., Wang, F., 2016. A modified SDS-based DNA extraction method for high quality environmental DNA from seafloor environments. Front. Microbiol. 7, 986. https://doi.org/10.3389/fmicb.2016.00986.
- Nguyen, L.T., Schmidt, H.A., von Haeseler, A., Minh, B.Q., 2015. IQ-TREE: a fast and effective stochastic algorithm for estimating maximum-likelihood phylogenies. Mol. Biol. Evol. 32 (1), 268–274. https://doi.org/10.1093/molbev/msu300.
- Parks, D.H., Imelfort, M., Skennerton, C.T., Hugenholtz, P., Tyson, G.W., 2015. CheckM: assessing the quality of microbial genomes recovered from isolates, single cells, and metagenomes. Genome Res. 25 (7), 1043–1055. https://doi.org/10.1101/gr.186077.114
- Peixoto, J., Silva, L.P., Kruger, R.H., 2017. Brazilian Cerrado soil reveals an untapped microbial potential for unpretreated polyethylene biodegradation. J. Hazard. Mater. 324 (Pt B), 634–644. https://doi.org/10.1016/j.jhazmat.2016.11.037.
- Peng, G., Zhu, B., Yang, D., Su, L., Shi, H., Li, D., 2017. Microplastics in sediments of the Changjiang Estuary, China. Environ. Pollut. 225 (4), 283–290. https://doi.org/ 10.1016/j.envpol.2016.12.064.
- Pinto, M., Zhao, Z., Klun, K., Libowitzky, E., Herndl, G.J., 2022. Microbial consortiums of putative degraders of low-density polyethylene-associated compounds in the ocean. mSystems 7 (2), e01415-01421. https://doi.org/10.1128/msystems.01415-21.
- Polz, M.F., Cavanaugh, C.M., 1998. Bias in template-to-product ratios in multitemplate PCR. Appl. Environ. Microbiol. 64 (10), 3724–3730. https://doi.org/10.1128/ AFM 64 10 3724-3730 1998
- Rabe von Pappenheim, F., Wensien, M., Ye, J., Uranga, J., Irisarri, I., de Vries, J., Funk, L. M., Mata, R.A., Tittmann, K., 2022. Widespread occurrence of covalent lysine-cysteine redox switches in proteins. Nat. Chem. Biol. 18 (4), 368–375. https://doi.org/10.1038/s41589-021-00966-5.
- Restrepo-Flórez, J.-M., Bassi, A., Thompson, M.R., 2014. Microbial degradation and deterioration of polyethylen—a review. Int. Biodeterior. Biodegrad. 88 (1), 83–90. https://doi.org/10.1016/j.ibiod.2013.12.014.

- Robert, X., Gouet, P., 2014. Deciphering key features in protein structures with the new ENDscript server. Nucleic Acids Res. 42 (Web Server issue), W320–W324. https:// doi.org/10.1093/nar/gku316.
- Rognes, T., Flouri, T., Nichols, B., Quince, C., Mahe, F., 2016. VSEARCH: a versatile open source tool for metagenomics. PeerJ 4, e2584. https://doi.org/10.7717/peerj.2584.
- Santo, M., Weitsman, R., Sivan, A., 2013. The role of the copper-binding enzyme-laccase—in the biodegradation of polyethylene by the actinomycete *Rhodococcus ruber*. Int. Biodeterior. Biodegrad. 84 (4), 204–210. https://doi.org/ 10.1016/j.ibiod.2012.03.001.
- Schmittgen, T.D., Livak, K.J., 2008. Analyzing real-time PCR data by the comparative C_T method. Nat. Protoc. 3 (6), 1101–1108. https://doi.org/10.1038/nprot.2008.73.
 Schrödinger, L., 2020. The PyMOL Molecular Graphics System, Version 2.4.0.
- Schwarz, A.E., Ligthart, T.N., Boukris, E., van Harmelen, T., 2019. Sources, transport, and accumulation of different types of plastic litter in aquatic environments: a review study. Mar. Pollut. Bull. 143 (4), 92–100. https://doi.org/10.1016/j.marpolbul.2019.04.029.
- Seemann, T., 2014. Prokka: rapid prokaryotic genome annotation. Bioinformatics 30 (14), 2068–2069. https://doi.org/10.1093/bioinformatics/btu153.
- Smith, B., 2021. The infrared spectra of polymers II: polyethylene. Spectroscopy 36 (9), 24–29. https://doi.org/10.56530/spectroscopy.xp7081p7.
- Sudhakar, M., Doble, M., Murthy, P.S., Venkatesan, R., 2008. Marine microbe-mediated biodegradation of low- and high-density polyethylenes. Int. Biodeterior. Biodegrad. 61 (3), 203–213. https://doi.org/10.1016/j.ibiod.2007.07.011.
- Tsiota, P., Karkanorachaki, K., Syranidou, E., Franchini, M., Kalogerakis, N., 2018. Microbial Degradation of HDPE Secondary Microplastics: Preliminary Results. Springer International Publishing, Cham, pp. 181–188. https://doi.org/10.1007/ 978.3.319.7129.6
- UNEP, 2021. From Pollution to Solution: A Global Assessment of Marine Litter and Plastic Pollution Reveals the Impact of Marine Litter and Plastic Pollution in the Environment and Their Effects on the Health of Ecosystems, Wildlife and Humans. Programme, U.N.E., Nairobi.
- Volke-Sepúlveda, T., Saucedo-Castañeda, G., Gutiérrez-Rojas, M., Manzur, A., Favela-Torres, E., 2002. Thermally treated low density polyethylene biodegradation by Penicillium pinophilum and Aspergillus niger. J. Appl. Polym. Sci. 83 (2), 305–314. https://doi.org/10.1002/app.2245.
- Wang, M.H., He, Y., Sen, B., 2019. Research and management of plastic pollution in coastal environments of China. Environ. Pollut. 248 (1), 898–905. https://doi.org/ 10.1016/j.envpol.2019.02.098.
- Watanabe, T., Ohtake, Y., Asabe, H., Murakami, N., Furukawa, M., 2009. Biodegradability and degrading microbes of low-density polyethylene. J. Appl. Polym. Sci. 111 (1), 551–559. https://doi.org/10.1002/app.29102.
- Wensien, M., von Pappenheim, F.R., Funk, L.M., Kloskowski, P., Curth, U., Diederichsen, U., Uranga, J., Ye, J., Fang, P., Pan, K.T., Urlaub, H., Mata, R.A., Sautner, V., Tittmann, K., 2021. A lysine-cysteine redox switch with an NOS bridge regulates enzyme function. Nature 593 (7859), 460–464. https://doi.org/10.1038/ s41586-021-03513-3.
- Wong, S.L., Ngadi, N., Abdullah, T.A.T., 2014. Study on dissolution of low density polyethylene (LDPE). Appl. Mech. Mater. 695, 170–173. https://doi.org/10.4028/ www.scientific.net/AMM.695.170.

- Xu, P., Peng, G., Su, L., Gao, Y., Gao, L., Li, D., 2018. Microplastic risk assessment in surface waters: a case study in the Changjiang Estuary, China. Mar. Pollut. Bull. 133 (1), 647–654. https://doi.org/10.1016/j.marpolbul.2018.06.020.
- Yang, J., Yang, Y., Wu, W.M., Zhao, J., Jiang, L., 2014. Evidence of polyethylene biodegradation by bacterial strains from the guts of plastic-eating waxworms. Environ. Sci. Technol. 48 (23), 13776–13784. https://doi.org/10.1021/es504038a.
- Yao, C., Xia, W., Dou, M., Du, Y., Wu, J., 2022a. Oxidative degradation of UV-irradiated polyethylene by laccase-mediator system. J. Hazard. Mater. 440, 129709 https:// doi.org/10.1016/j.jhazmat.2022.129709.
- Yao, Z., Seong, H.J., Jang, Y.S., 2022b. Environmental toxicity and decomposition of polyethylene. Ecotoxicol. Environ. Saf. 242, 113933 https://doi.org/10.1016/j. ecoeny. 2022.113933
- Yoon, G.M., Jeon, J.H., Kim, N.M., 2012. Biodegradation of polyethylene by a soil bacterium and alkB cloned recombinant cell. J. Bioremed. Biodegrad. 3 (4), 1000144. https://doi.org/10.4172/2155-6199.1000145.
- Yoon, S.H., Ha, S.M., Kwon, S., Lim, J., Kim, Y., Seo, H., Chun, J., 2017. Introducing EzBioCloud: a taxonomically united database of 16S rRNA gene sequences and whole-genome assemblies. Int. J. Syst. Evol. Microbiol. 67 (5), 1613–1617. https://doi.org/10.1099/jisem.0.001755
- Yoshida, S., Hiraga, K., Takehana, T., Taniguchi, I., Yamaji, H., Maeda, Y., Toyohara, K., Miyamoto, K., Kimura, Y., Oda, K., 2016. A bacterium that degrades and assimilates poly(ethylene terephthalate). Science 351 (6278), 1196. https://doi.org/10.1126/ science.aad6359.
- Yuan, J., Ma, J., Sun, Y., Zhou, T., Zhao, Y., Yu, F., 2020. Microbial degradation and other environmental aspects of microplastics/plastics. Sci. Total Environ. 715, 136968 https://doi.org/10.1016/j.scitotenv.2020.136968.
- Zadjelovic, V., Erni-Cassola, G., Obrador-Viel, T., Lester, D., Eley, Y., Gibson, M.I., Dorador, C., Golyshin, P.N., Black, S., Wellington, E.M.H., Christie-Oleza, J.A., 2022. A mechanistic understanding of polyethylene biodegradation by the marine bacterium Alcanivorax. J. Hazard. Mater. 436, 129278 https://doi.org/10.1016/j. jhazmat.2022.129278.
- Zampolli, J., Orro, A., Manconi, A., Ami, D., Natalello, A., Di Gennaro, P., 2021.
 Transcriptomic analysis of *Rhodococcus opacus* R7 grown on polyethylene by RNA-seq. Sci. Rep. 11 (1), 21311. https://doi.org/10.1038/s41598-021-00525-x.
- Zhang, W.J., He, Y.X., Yang, Z., Yu, J., Chen, Y., Zhou, C.Z., 2008. Crystal structure of glutathione-dependent phospholipid peroxidase Hyr1 from the yeast Saccharomyces cerevisiae. Proteins 73 (4), 1058–1062. https://doi.org/10.1002/prot.22220.
- Zhang, C., Zhou, H., Cui, Y., Wang, C., Li, Y., Zhang, D., 2019. Microplastics in offshore sediment in the Yellow Sea and East China Sea, China. Environ. Pollut. 244, 827–833. https://doi.org/10.1016/j.envpol.2018.10.102.
- Zhang, Y., Lin, Y., Gou, H., Feng, X., Zhang, X., Yang, L., 2022. Screening of polyethylene-degrading bacteria from *Rhyzopertha Dominica* and evaluation of its key enzymes degrading polyethylene. Polymers (Basel) 14 (23). https://doi.org/ 10.3390/polym14235127.
- Zhang, X., Feng, X., Lin, Y., Gou, H., Zhang, Y., Yang, L., 2023. Degradation of polyethylene by *Klebsiella pneumoniae* Mk-1 isolated from soil. Ecotoxicol. Environ. Saf. 258, 114965 https://doi.org/10.1016/j.ecoenv.2023.114965.
- Zhao, S., Wang, T., Zhu, L., Xu, P., Wang, X., Gao, L., Li, D., 2019. Analysis of suspended microplastics in the Changjiang Estuary: implications for riverine plastic load to the ocean. Water Res. 161, 560–569. https://doi.org/10.1016/j.watres.2019.06.019.